Secure Massive MIMO Relaying Systems in a Poisson Field of Eavesdroppers

Tiep M. Hoang, *Student Member, IEEE*, Trung Q. Duong, *Senior Member, IEEE*, Hoang Duong Tuan, and H. Vincent Poor, *Fellow, IEEE*

***Abstract*— A cooperative relay network operating in the presence of eavesdroppers, whose locations are distributed according to a homogeneous Poisson point process, is considered. The relay is equipped with a very large antenna array and can exploit maximal ratio combing in the uplink and maximal ratio transmission in the downlink. A realistic model in which the channel state information of every eavesdropper is not known is considered, as eavesdroppers tend to hide themselves in practice. The destination is thus in a much weaker position than all the eavesdroppers because it only receives the retransmitted signal from the relay. Under this setting, the security performance is investigated for two relaying protocols: amplify-and-forward and decode-and-forward. The secrecy outage probability, the connection outage probability, and the tradeoff between them, which is controlled by the source power allocation, are examined. Finally, suitable solutions for the source power (such that once the transmission occurs with high reliability, the secure risk is below a given threshold) are proposed for a tradeoff between security and reliability.**

***Index Terms*— Security, massive MIMO, Poisson point process, maximal-ratio combining, maximal-ratio transmission, amplify-and-forward, decode-and-forward.**

I. Introduction

PHYSICAL layer security (PLS) has attracted considerable attention from both academia and industry in recent years [1]. With the recent emergence of large antenna arrays [2], PLS is a promising approach for massive multiple-input multiple-output (MIMO) systems as countermeasures against eavesdropping attacks. Noticeably, the desired characteristics of massive MIMO systems are not present in conventional systems with small antenna arrays, e.g. an inner product of two random vectors can converge in distribution. Indeed, massive MIMO systems have been demonstrated to improve secure performance in several studies [3]–[12]. Having said that, the role of massive MIMO systems in preventing eavesdroppers is not yet completely understood, mainly because PLS contains relatively many distinct aspects such as artificial noise (AN) techniques, antenna/relay/jammer/user selection techniques, and strategies to deal with the leakage of information. Moreover, different combinations of secure and relaying techniques also make security scenarios more diverse. Thus, the issue of security in massive MIMO relaying systems is still largely open.

Additionally, it is should be mentioned that the assumptions made about of eavesdroppers are of crucial importance. Notably, since the locations of eavesdroppers is typically not known, many authors have taken into account the spatial distribution of eavesdroppers by adopting a spatial point process model. For example, in order to model the spatial location of eavesdroppers, Wang and Wang [13], Wang *et al.* [14], and Chae *et al.* [15] used a homogeneous Poisson point process (PPP) model because of its mathematical tractability. It should also be noted that in the context of stochastic geometry, the PPP is the most widely used and important point process to describe spatially distributed discrete nodes [16]–[18]. Thus, the PPP will be adopted to model the spatial location of eavesdroppers in this paper.

Among recent works on security for massive MIMO relaying systems [3]–[8], Chen *et al.* [3], [4] considered cooperative relay systems and compared the security improvement for both amplify-and-forward (AF) and decode-and-forward (DF) relaying, while only the AF scheme (or the DF scheme) was considered in [5] and [6] (or in [7] and [8]). These works, however, did not consider any direct link between source and eavesdropper. Note that in general, eavesdroppers may possibly receive two versions of transmitted messages from the source and relay in cooperative relay networks. Thus, the lack of consideration of direct links in [3]–[8] could lead to an incomplete understanding of the ways in which eavesdroppers can benefit from the configuration of cooperative relay networks. On the other hand, the impact of a direct eavesdropping link on the secure performance of relay networks was presented in [19], but there was no discussion of large antenna arrays. Finally, other recent papers on secure massive MIMO networks (not necessarily relay-aided networks) can be also found in the literature (e.g. [9]–[12]) in the context of the impact of the so-called *pilot contamination* scheme in which an eaves-

Manuscript received December 23, 2016; revised April 13, 2017 and June 6, 2017; accepted June 26, 2017. Date of publication July 5, 2017; date of current version November 15, 2017. This work was supported in part by the U.K. Royal Academy of Engineering Research Fellowship under Grant RF1415\14\22 and by the U.K. Engineering and Physical Sciences Research Council (EPSRC) under Grant EP/P019374/1, in part by the Australian Research Councils Discovery Projects under Project DP130104617, and in part by the U.S. National Science Foundation under Grants CMMI-1435778, ECCS-1549881 and ECCS-1647198. This paper was presented at the IEEE 85th Vehicular Technology Conference (VTC-Spring) in 2017. The associate editor coordinating the review of this paper and approving it for publication was K. Tourki. *(Corresponding author: Trung Q. Duong.)*

T. M. Hoang and T. Q. Duong are with the School of Electronics, Electrical Engineering and Computer Science, Queen's University Belfast, Belfast BT7 1NN, U.K. (e-mail: mhoang02@qub.ac.uk; trung.q.duong@qub.ac.uk).

H. D. Tuan is with the Faculty of Engineering and Information Technology, University of Technology Sydney, Ultimo, NSW, Australia (e-mail: tuan.hoang@uts.edu.au).

H. V. Poor is with the Department of Electrical Engineering, Princeton University, Princeton, NJ 08544 USA (e-mail: poor@princeton.edu).

Color versions of one or more of the figures in this paper are available online at http://ieeexplore.ieee.org.

Digital Object Identifier 10.1109/TCOMM.2017.2723565

dropper can send a pilot sequence to attack massive MIMO systems, but this issue is beyond the scope of our paper.[1] Note that none of the above studies (i.e. [3]–[12]) have considered the spatial locations of eavesdroppers as a whole and the impact of direct eavesdropping links in particular.

On the contrary, the works in [13]–[15] considered the same assumption of the eavesdroppers' spatial distribution as in this work, but the topic of large antenna arrays was not discussed. For example, [13] analyzed the secure performance for millimeter wave systems instead of massive MIMO systems. While Wang *et al.* [14] and Chae *et al.* [15] used artificial noise instead of large antenna arrays to deal with eavesdropping attacks. Given that the artificial noise technique is also a signal generation process, the additional complexity it adds may not be necessary for large-scale antenna systems, because such systems themselves can provide considerable benefits in terms of security [4]. Aiming to investigate the joint impact of massive MIMO systems and eavesdroppers' geometric locations on the secure performance, [20] analyzed the secrecy outage probability (SOP) with emphasis on the potential locations of eavesdroppers. However, eavesdroppers in [20] are assumed to be uniformly distributed with a fixed number of eavesdroppers. Such an assumption may be unreasonable for wireless systems which typically do not have the knowledge of the number of eavesdroppers. It is clear that the assumption of PPP-distributed eavesdroppers has not yet been adopted for secure massive MIMO systems as a whole, and secure massive MIMO relaying systems in particular.

In short, the works on security (mentioned in the above paragraphs) have analyzed either massive MIMO systems without using a PPP model for eavesdropper locations, or conventional MIMO systems with the use of such a PPP model. Thus, our work fills this gap by adopting the more realistic assumption of PPP-distributed eavesdroppers for cooperative wireless systems with large antenna arrays. In this paper, we consider a secure wireless network with the aid of a large antenna array at an intermediate relay. As for the relaying protocol, we consider conventional relaying schemes like AF and DF for comparison purposes, instead of delving into more recently-developed relaying schemes (e.g. [21]). Around the relay, there exist many potential eavesdroppers whose locations are assumed to follow a PPP; thus, we must take the direct links between source and eavesdroppers into account. On the hand, the direct link between source and destination is assumed to be impaired and neglected. Intuitively, all potential eavesdroppers can take advantage of the fact that they receive two versions of confidential signals. To quantify how harmful the eavesdroppers can be, we evaluate the secure performance by using the SOP. Then we use an ON-OFF scheme for the transmission in which the source transmits its messages only when the legitimate channels are strong enough (i.e. reliable enough). To elucidate how reliable the secure transmission can be, we evaluate the performance by using the connection outage probability (COP). Finally, based on the SOP and the COP, we examine the state in which our system is the most secure, and show that this state can be achieved when the source power is just slightly larger than a certain threshold (as long as the COP reaches 0). We also derive asymptotic expressions for the SOP and the COP for each relaying strategy. We observe that if the ratio of the average transmit power at the source to the average noise power at the destination is high, the security of the proposed system seems to depend on only the eavesdroppers' working range as well as the intensity of their presence. We also observe that when the source power increases, the SOP reaches its largest limit, while the COP equals 0. Moreover, for both relaying protocols, the reliability of the system is demonstrated to gain from increasing the number of antennas. Finally, our numerical results show the agreement between analysis and simulation.

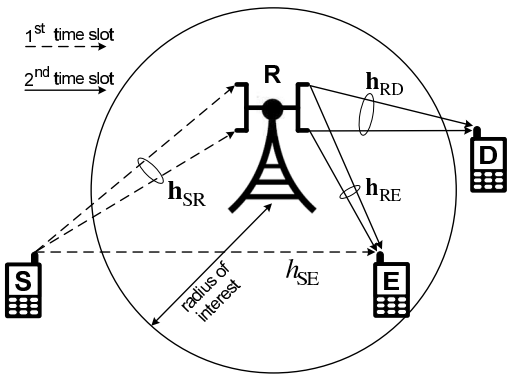

Fig. 1. System model.

The remainder of this paper is organized as follows: Section II describes the network configuration and restricts the case study to the worst case. In Section III, we provide the approximate characterization of the received signal-to-noise ratios (SNRs) assuming a large antenna array. Sections IV and V derive exact and asymptotic expressions for the SOP and the COP, respectively. In Section VI, optimization problems are suggested for the AF and DF cases in order to improve the secure performance. Numerical results are shown in Section VII and finally, conclusions are provided in Section VIII.

Notation: $[\cdot]^T$, $[\cdot]^*$, and $[\cdot]^\dagger$ denote the transpose operator, conjugate operator, and Hermitian operator, respectively. Vectors and matrices are represented with lowercase boldface and uppercase boldface, respectively. $\mathbf{I}_n$ is the $n \times n$ identity matrix. $\|\cdot\|$ denotes the Euclidean norm. $\mathbb{E}\{\cdot\}$ denotes expectation. $\mathbf{z} \sim \mathcal{CN}_n(\mathbf{\Sigma})$ denotes a complex Gaussian vector $\mathbf{z} \in \mathbb{C}^{n\times 1}$ with zero-mean and covariance matrix $\mathbf{\Sigma} \in \mathbb{C}^{n\times n}$. $\mathsf{Exp}(r)$ denotes the exponential distribution with rate r.

II. System Model

As shown in Fig. 1, we consider a cooperative relay network in which there is a single source (S), a trusted relay (R), a destination (D), and multiple passive eavesdroppers (Ei with $i = 1, 2, \ldots$).[2] The distance between S and D is very large so that R is invoked to help convey messages from S to D.

[1]The context of pilot contamination can be ignored when considering a single cell, and especially when the pilot training only accounts for a very small portion of each coherence interval.

[2]We consider a practical scenario in which each eavesdropper hides itself, and thus all eavesdroppers are passive.

As such, it is reasonable to assume that there is no direct link between S and D. However, the direct link between S and Ei is taken into account since Ei is likely to be present around S and/or R to overhear some confidential messages. We assume that R is equipped with a very large receive antenna array to decode its received signal in the uplink and a very large transmit antenna array to forward its decoded signal in the downlink; meanwhile, each of the remaining nodes (i.e. S, D and Ei) has only one antenna. It should be noted that both the number of transmit antennas and the number of receive antennas at R are equal to $N \gg 2$. The eavesdroppers are assumed to be spatially distributed according to a homogeneous PPP Ψ with intensity $\lambda > 0$, and yet they are only present within a circle $\mathcal{B}(R_\Psi R_0)$, which is centered at the origin R with the radius $R_\Psi R_0$.[3] By keeping silent to avoid being detected, eavesdroppers do not get involved in actions like attacking pilot sequences.

Regarding the propagation model, we consider both small-scale and large-scale fading factors. The small-scale fading is characterized by $\mathbf{h}_{\mathrm{XY}} \in \mathbb{C}^{n\times 1}$ $\left(\text{or } \mathbf{h}_{\mathrm{XY}}^T \in \mathbb{C}^{n\times 1}\right)$ with its magnitude being Rayleigh distributed. We assume that the column vector $\mathbf{h}_{\mathrm{XY}}$ $\left(\text{or } \mathbf{h}_{\mathrm{XY}}^T\right)$ is distributed according to $\mathcal{CN}_n(\mathbf{I}_n)$. The large-scale fading is characterized by $l_{\mathrm{XY}}^{-\alpha/2}$ with $\alpha > 2$ being the path-loss exponent and $l_{\mathrm{XY}} R_0$ being the length of the X$-$Y link. In path loss models [22]–[24], l_{XY} is understood as the ratio of the real distance to R_0. For example, R_0 is often taken to be 100 m for microcells [24], in which case $l_{\mathrm{XY}} = 2$ means that the real distance between X and Y is $2R_0 = 200$ m.

To facilitate the analysis, we use polar coordinates with R being the origin (as aforementioned) and ϕ being the angle $\widehat{\mathrm{SRE}i}$. Then we have $l_{\mathrm{SE}} = \sqrt{L_{\mathrm{SR}}^2 + l^2 - 2L_{\mathrm{SR}} l\cos\phi}$ with $L_{\mathrm{SR}} \equiv l_{\mathrm{SR}}$, $L_{\mathrm{RD}} \equiv l_{\mathrm{RD}}$ and $l \equiv l_{\mathrm{RE}}$. Obviously, l_{SE} is a function of l and ϕ due to the random spatial distribution of Ei.

Regarding transmission, we use two equal time slots. In the first time slot, S transmits the source signal $s \in \mathbb{C}$ to R. In the second time slot, S keeps silent while R forwards the relaying signal $\mathbf{r} \in \mathbb{C}^{N\times 1}$ to D. In these two phases, both the signal transmitted from S (i.e. s) and the signal retransmitted from R (i.e. $\mathbf{r}$) are overheard by Ei.

- We normalize s such that $\mathbb{E}\left\{|s|^2\right\} = 1$, and then the signals received at R and Ei in the first time slot are, respectively, written as

$$\mathbf{y}_{\mathrm{R}} = \sqrt{\gamma_{\mathrm{S}}} L_{\mathrm{SR}}^{-\alpha/2} \mathbf{h}_{\mathrm{SR}} s + \mathbf{n}_{\mathrm{R}}, \tag{1}$$

$$y_{\mathrm{E},1} = \sqrt{\gamma_{\mathrm{S}}} l_{\mathrm{SE}}^{-\alpha/2} h_{\mathrm{SE}} s + n_{\mathrm{E},1} \tag{2}$$

  where $\mathbf{n}_{\mathrm{R}} \sim \mathcal{CN}_N(\mathbf{I}_N)$ and $n_{\mathrm{E},1} \sim \mathcal{CN}_1(1)$ are additive white Gaussian noises (AWGNs) at R and Ei, respectively; and $L_{\mathrm{SR}}^{-\alpha/2}\mathbf{h}_{\mathrm{SR}} \in \mathbb{C}^{N\times 1}$ and $l_{\mathrm{SE}}^{-\alpha/2} h_{\mathrm{SE}} \in \mathbb{C}$ are the complex channel coefficients for the S-R and S-Ei links. γ_{S} is the average received SNR per antenna at R as well as the average received SNR at Ei. Note that the average noise power is assumed to be the same at every receive antenna.

- We normalize $\mathbf{r}$ such that $\mathbb{E}\left\{\mathbf{r}\mathbf{r}^\dagger\right\} = \mathbf{I}_N$, and then the signals received at D and Ei in the second time slot are, respectively, written as

$$y_{\mathrm{D}} = \sqrt{\gamma_{\mathrm{R}}/N} L_{\mathrm{RD}}^{-\alpha/2} \mathbf{h}_{\mathrm{RD}}^T \mathbf{r} + n_{\mathrm{D}}, \tag{3}$$

$$y_{\mathrm{E},2} = \sqrt{\gamma_{\mathrm{R}}/N} l^{-\alpha/2} \mathbf{h}_{\mathrm{RE}}^T \mathbf{r} + n_{\mathrm{E},2} \tag{4}$$

  where $n_{\mathrm{D}} \sim \mathcal{CN}_1(1)$ and $n_{\mathrm{E},2} \sim \mathcal{CN}_1(1)$ are AWGNs at D and Ei, respectively; and $L_{\mathrm{RD}}^{-\alpha/2}\mathbf{h}_{\mathrm{RD}} \in \mathbb{C}^{1\times N}$ and $l^{-\alpha/2}\mathbf{h}_{\mathrm{RE}} \in \mathbb{C}^{1\times N}$ are the complex channel coefficients the R-D and R-Ei links. γ_{R} is the average received SNR at D as well as at Ei.

We note that for the sake of simplicity, the average noise power is assumed to be the same at every receive antenna. This leads to the fact that both (1) and (2) contain the same γ_{S}, while both (3) and (4) contain the same γ_{R}. With the noise normalization, γ_{S} is both the average received SNR per antenna at R and the average received SNR at Ei, while γ_{R} is the average received SNR at D as well as Ei. It should also be noted that the subscript $[\cdot]_{\mathrm{E}}$ is implicitly related to Ei with $i \in \Psi$; however, the index i is dropped for notational convenience.

A. MRC/MRT at the Relay

After being received at R, the signal $\mathbf{y}_{\mathrm{R}}$ is then multiplied by a weighting vector $\mathbf{w}^\dagger \in \mathbb{C}^{1\times N}$ to combine the N received signals in (1) using maximal-ratio combing (MRC). Moreover, in the uplink, $\mathbf{w}$ is designed only based on $\mathbf{h}_{\mathrm{SR}}$ because the instantaneous h_{SE} is not known (i.e. there is no channel state information (CSI) for the eavesdroppers).[4] Hence, according to the MRC principle, we have $\mathbf{w} = \mathbf{h}_{\mathrm{SR}}/\|\mathbf{h}_{\mathrm{SR}}\|$. The obtained signal after this process can be written as

$$r_0 = \mathbf{w}^\dagger \mathbf{y}_{\mathrm{R}} = \sqrt{\gamma_{\mathrm{S}}} L_{\mathrm{SR}}^{-\alpha/2} \|\mathbf{h}_{\mathrm{SR}}\| s + \frac{\mathbf{h}_{\mathrm{SR}}^\dagger}{\|\mathbf{h}_{\mathrm{SR}}\|} \mathbf{n}_{\mathrm{R}}. \tag{5}$$

The MRC output signal r_0 is then processed by R according to the chosen relaying protocol (i.e., AF or DF). Then, the obtained signal $\widehat{r}_0$ is multiplied by another weighting vector $\mathbf{v} \in \mathbb{C}^{N\times 1}$ to form the retransmitted signal $\mathbf{r}$. In the same way as the design of $\mathbf{w}$, the weighting vector $\mathbf{v}$ is designed only based on $\mathbf{h}_{\mathrm{RD}}$. As such, applying maximal-ratio transmission (MRT) to the downlink, we have $\mathbf{v} = \mathbf{h}_{\mathrm{RD}}^*/\|\mathbf{h}_{\mathrm{RD}}\|$. Hence, the relation between the decoded signal $\widehat{r}_0$ and the retransmitted signal $\mathbf{r}$ is given by

$$\mathbf{r} = \mathbf{v}\widehat{r}_0 = \frac{\mathbf{h}_{\mathrm{RD}}^*}{\|\mathbf{h}_{\mathrm{RD}}\|}\widehat{r}_0. \tag{6}$$

In the following, the expressions for $\widehat{r}_0$ will be discussed for the two different relaying operations, namely, AF and DF.

1) AF at R: In this case, the signal $\widehat{r}_0$ is simply a scaled version of the signal r_0, i.e.

$$\widehat{r}_0 = c^{AF} r_0 \tag{7}$$

[3] It is important to note that if λ is measured by the average number of eavesdroppers over the area of R_0^2, then the average number of eavesdroppers within the circle $\mathcal{B}(R_\Psi R_0)$ is calculated as $\lambda \int_0^{R_\Psi} \int_0^{2\pi} l d l d\phi$ but not $\lambda \int_0^{R_\Psi R_0} \int_0^{2\pi} l d l d\phi$. Herein, R_0 is referred to as a reference distance, while R_Ψ is the ratio of the real radius to R_0. For example, if we have $R_0 = 1$ km and $R_\Psi = 2$, the radius of the considered circle will be 2 km.

[4] Since the design of $\mathbf{w}$ does not take $\mathbf{h}_{\mathrm{SE}}$ into account due to the lack of the CSI of Ei, the design of $\mathbf{w}$ according to the MRC principle is not the optimal solution in terms of security.

where c^{AF} is a constant subject to the following transmit power constraint:

$$\mathrm{tr}\left(\mathbb{E}\left\{\mathbf{r}\mathbf{r}^{\dagger}\right\}\right) = \mathrm{tr}\left(\mathbf{I}_N\right) = N. \tag{8}$$

Using (5)–(8) yields

$$c^{AF} = \sqrt{\frac{N}{\gamma_{\mathrm{S}} L_{\mathrm{SR}}^{-\alpha} \|\mathbf{h}_{\mathrm{SR}}\|^2 + 1}}. \tag{9}$$

Substituting (5) and (9) into (6)–(7), we obtain a new expression for $\mathbf{r}$ and then again substituting this new expression into (3)–(4), we can rewrite (3)–(4) as

$$y_{\mathrm{D}}^{AF} = \sqrt{\frac{\gamma_{\mathrm{S}}\gamma_{\mathrm{R}} L_{\mathrm{SR}}^{-\alpha} L_{\mathrm{RD}}^{-\alpha} \|\mathbf{h}_{\mathrm{SR}}\|^2}{\gamma_{\mathrm{S}} L_{\mathrm{SR}}^{-\alpha} \|\mathbf{h}_{\mathrm{SR}}\|^2 + 1}} \|\mathbf{h}_{\mathrm{RD}}\| s + n_{\mathrm{D}}^{AF}, \tag{10}$$

$$y_{\mathrm{E},2}^{AF} = \sqrt{\frac{\gamma_{\mathrm{S}}\gamma_{\mathrm{R}} L_{\mathrm{SR}}^{-\alpha} l^{-\alpha} \|\mathbf{h}_{\mathrm{SR}}\|^2}{\gamma_{\mathrm{S}} L_{\mathrm{SR}}^{-\alpha} \|\mathbf{h}_{\mathrm{SR}}\|^2 + 1}} \frac{\mathbf{h}_{\mathrm{RE}}^T \mathbf{h}_{\mathrm{RD}}^*}{\|\mathbf{h}_{\mathrm{RD}}\|} s + n_{E,2}^{AF} \tag{11}$$

where

$$n_{\mathrm{D}}^{AF} \triangleq \sqrt{\frac{\gamma_{\mathrm{R}} L_{\mathrm{RD}}^{-\alpha} \|\mathbf{h}_{\mathrm{RD}}\|^2}{\gamma_{\mathrm{S}} L_{\mathrm{SR}}^{-\alpha} \|\mathbf{h}_{\mathrm{SR}}\|^2 + 1}} \frac{\mathbf{h}_{\mathrm{SR}}^{\dagger}}{\|\mathbf{h}_{\mathrm{SR}}\|} \mathbf{n}_{\mathrm{R}} + n_{\mathrm{D}}, \tag{12}$$

$$n_{\mathrm{E},2}^{AF} \triangleq \sqrt{\frac{\gamma_{\mathrm{R}} l^{-\alpha}}{\gamma_{\mathrm{S}} L_{\mathrm{SR}}^{-\alpha} \|\mathbf{h}_{\mathrm{SR}}\|^2 + 1}} \frac{\mathbf{h}_{\mathrm{RE}}^T \mathbf{h}_{\mathrm{RD}}^* \mathbf{h}_{\mathrm{SR}}^{\dagger}}{\|\mathbf{h}_{\mathrm{RD}}\| \|\mathbf{h}_{\mathrm{SR}}\|} \mathbf{n}_{\mathrm{R}} + n_{\mathrm{E},2}. \tag{13}$$

2) DF at R: In this case, we consider the case in which both the source and the relay use the same codeword for their transmission [25]. The signal $\widehat{r}_0$ is successfully decoded from the signal r_0, and thus we have the following relation:

$$\widehat{r}_0 = c^{DF} s, \tag{14}$$

where c^{DF} is a constant subject to the constraint (8). From (6), (8) and (14), we have $c^{DF} = \sqrt{N}$ whereby (6) can be written as

$$\mathbf{r} = \frac{\mathbf{h}_{\mathrm{RD}}^*}{\|\mathbf{h}_{\mathrm{RD}}\|} \sqrt{N} s. \tag{15}$$

Substituting the above expression into (3)–(4), we can rewrite (3)–(4) as

$$y_{\mathrm{D}}^{DF} = \sqrt{\gamma_{\mathrm{R}}} L_{\mathrm{RD}}^{-\alpha/2} \|\mathbf{h}_{\mathrm{RD}}\| s + n_{\mathrm{D}}, \tag{16}$$

$$y_{\mathrm{E},2}^{DF} = \sqrt{\gamma_{\mathrm{R}}} l^{-\alpha/2} \frac{\mathbf{h}_{\mathrm{RE}}^T \mathbf{h}_{\mathrm{RD}}^*}{\|\mathbf{h}_{\mathrm{RD}}\|} s + n_{\mathrm{E},2}. \tag{17}$$

B. Signal-to-Noise Ratios in the Worst Case

We assume that each Ei is capable of exploiting the best possible decoding strategy to maximize its received signals. Herein, we suppose that Ei is able to use MRC to combine one signal from S and N signals from R. Obviously, the strategy for the eavesdroppers will differ depending on whether the relay is using AF or DF.

1) AF at R: From (2) and (11), the overall received signals at Ei can be written as

$$\mathbf{y}_{\mathrm{E}}^{AF} = \underbrace{\begin{bmatrix} \sqrt{\gamma_{\mathrm{S}}} l_{\mathrm{SE}}^{-\alpha/2} h_{\mathrm{SE}} \\ \sqrt{\frac{\gamma_{\mathrm{S}}\gamma_{\mathrm{R}} L_{\mathrm{SR}}^{-\alpha} l^{-\alpha} \|\mathbf{h}_{\mathrm{SR}}\|^2}{\gamma_{\mathrm{S}} L_{\mathrm{SR}}^{-\alpha} \|\mathbf{h}_{\mathrm{SR}}\|^2 + 1}} \frac{\mathbf{h}_{\mathrm{RE}}^T \mathbf{h}_{\mathrm{RD}}^*}{\|\mathbf{h}_{\mathrm{RD}}\|} \end{bmatrix}}_{\triangleq \mathbf{g}^{AF}} s + \underbrace{\begin{bmatrix} n_{\mathrm{E},1} \\ n_{E,2}^{AF} \end{bmatrix}}_{\triangleq \widetilde{\mathbf{n}}^{AF}}. \tag{18}$$

Then using MRC receiver with the weighting vector $\mathbf{f}^{AF}$, we can write the combined output at Ei as

$$z_{\mathrm{E}}^{AF} = \left(\mathbf{f}^{AF}\right)^{\dagger} \mathbf{g}^{AF} s + \left(\mathbf{f}^{AF}\right)^{\dagger} \widetilde{\mathbf{n}}^{AF}. \tag{19}$$

From (19), the instantaneous SNR at Ei can be generally written as [26][5]

$$\widehat{\mathrm{SNR}}_{\mathrm{E}}(\mathbf{f}^{AF}) = \frac{\left(\mathbf{f}^{AF}\right)^{\dagger} \left(\mathbf{g}^{AF} \left(\mathbf{g}^{AF}\right)^{\dagger}\right) \mathbf{f}^{AF}}{\left(\mathbf{f}^{AF}\right)^{\dagger} \widetilde{\mathbf{R}}^{AF} \mathbf{f}^{AF}} \leq \left(\mathbf{g}^{AF}\right)^{\dagger} \left(\widetilde{\mathbf{R}}^{AF}\right)^{-1} \mathbf{g}^{AF} \tag{20}$$

where $\widetilde{\mathbf{R}}^{AF}$ is the covariance matrix of $\widetilde{\mathbf{n}}^{AF}$. The equality in (20) holds for

$$\mathbf{f}^{AF} = \tau \left(\widetilde{\mathbf{R}}^{AF}\right)^{-1} \mathbf{g}^{AF} \triangleq \mathbf{f}_{opt}^{AF} \tag{21}$$

with τ being an arbitrary constant. It is apparent that in practice, a wise Ei is likely to design $\mathbf{f}^{AF} = \mathbf{f}_{opt}^{AF}$ to maximize its received SNR. Taking this into account, we assume that the received SNR at Ei is

$$\widehat{\mathrm{SNR}}_{\mathrm{E}} \equiv \widehat{\mathrm{SNR}}_{\mathrm{E}}(\mathbf{f}_{opt}^{AF}) = \left(\mathbf{g}^{AF}\right)^{\dagger} \left(\widetilde{\mathbf{R}}^{AF}\right)^{-1} \mathbf{g}^{AF}. \tag{22}$$

As such, we will only discuss this practical scenario throughout the rest of this paper.

The covariance matrix of $\widetilde{\mathbf{n}}^{AF}$ in (18) can be expressed as

$$\widetilde{\mathbf{R}}^{AF} = \mathbb{E}\left\{\widetilde{\mathbf{n}}^{AF} \left(\widetilde{\mathbf{n}}^{AF}\right)^{\dagger}\right\} = \begin{bmatrix} 1 & 0 \\ 0 & \dfrac{\gamma_{\mathrm{R}} l^{-\alpha} |\mathbf{h}_{\mathrm{RD}}^T \mathbf{h}_{\mathrm{RE}}^*|^2}{\left(\gamma_{\mathrm{S}} L_{\mathrm{SR}}^{-\alpha} \|\mathbf{h}_{\mathrm{SR}}\|^2 + 1\right) \|\mathbf{h}_{\mathrm{RD}}\|^2} + 1 \end{bmatrix}. \tag{23}$$

Substituting $\mathbf{g}^{AF}$ in (18) and $\widetilde{\mathbf{R}}^{AF}$ in (23) into (22), we can write the instantaneous SNR at Ei in the case of AF as

$$\widehat{\mathrm{SNR}}_{\mathrm{E}}^{AF} = \frac{\gamma_{\mathrm{S}} L_{\mathrm{SR}}^{-\alpha} \gamma_{\mathrm{R}} l^{-\alpha} \|\mathbf{h}_{\mathrm{SR}}\|^2 |\mathbf{h}_{\mathrm{RD}}^T \mathbf{h}_{\mathrm{RE}}^*|^2}{\left(\gamma_{\mathrm{S}} L_{\mathrm{SR}}^{-\alpha} \|\mathbf{h}_{\mathrm{SR}}\|^2 + 1\right) \|\mathbf{h}_{\mathrm{RD}}\|^2 + \gamma_{\mathrm{R}} l^{-\alpha} |\mathbf{h}_{\mathrm{RD}}^T \mathbf{h}_{\mathrm{RE}}^*|^2 + \gamma_{\mathrm{S}} l_{\mathrm{SE}}^{-\alpha} |h_{\mathrm{SE}}|^2}. \tag{24}$$

From (10), the instantaneous SNR at D can be written as

$$\widehat{\mathrm{SNR}}_{\mathrm{D}}^{AF} = \frac{\gamma_{\mathrm{S}} L_{\mathrm{SR}}^{-\alpha} \gamma_{\mathrm{R}} L_{\mathrm{RD}}^{-\alpha} \|\mathbf{h}_{\mathrm{SR}}\|^2 \|\mathbf{h}_{\mathrm{RD}}\|^2}{\gamma_{\mathrm{S}} L_{\mathrm{SR}}^{-\alpha} \|\mathbf{h}_{\mathrm{SR}}\|^2 + \gamma_{\mathrm{R}} L_{\mathrm{RD}}^{-\alpha} \|\mathbf{h}_{\mathrm{RD}}\|^2 + 1}. \tag{25}$$

[5]Since the term $\widetilde{\mathbf{R}}^{AF}$ in (20) is positive definite, we can factorize it into $\mathbf{U}^{\dagger}\mathbf{U}$ by using Cholesky decomposition. The left hand side of (20) can be rewritten as $\widehat{\mathrm{SNR}}_{\mathrm{E}}(\mathbf{f}_0) = \left[\mathbf{f}_0^{\dagger}\left(\mathbf{g}_0\mathbf{g}_0^{\dagger}\right)\mathbf{f}_0\right] \Big/ \left(\mathbf{f}_0^{\dagger}\mathbf{f}_0\right)$ where $\mathbf{f}_0 \triangleq \mathbf{U}\mathbf{f}^{AF} \in \mathbb{C}^{2\times 1}$ and $\mathbf{g}_0 \triangleq \left(\mathbf{U}^{\dagger}\right)^{-1} \mathbf{g}^{AF} \in \mathbb{C}^{2\times 1}$. Obviously, the new expression for the instantaneous SNR at Ei with respect to $\mathbf{f}_0$ is now a Rayleigh quotient [27]–[28]; therefore we have $\max_{\mathbf{f}_0} \widehat{\mathrm{SNR}}_{\mathrm{E}}(\mathbf{f}_0) = \lambda_{\max}\left(\mathbf{g}_0\mathbf{g}_0^{\dagger}\right) = \|\mathbf{g}_0\|^2$ where $\lambda_{\max}$ is the maximum eigenvalue of $\mathbf{g}_0\mathbf{g}_0^{\dagger}$, and the last equality follows from the fact that $\mathbf{g}_0\mathbf{g}_0^{\dagger}$ has rank one. Then the right hand side of (20) is obtained by substituting $\mathbf{g}_0 = \left(\mathbf{U}^{\dagger}\right)^{-1} \mathbf{g}^{AF}$ and $\mathbf{U}^{\dagger}\mathbf{U} = \widetilde{\mathbf{R}}^{AF}$.

2) DF at R: Expressions for the SNRs for the DF scheme are formulated differently from those for the AF scheme. When only considering the indirect transmission from S to D through R, we can infer the instantaneous SNR at Ei from (1) and (17) as follows [29]:

$$\widehat{\mathrm{SNR}}_{\mathrm{E,\ indirect}}^{DF} = \min\left\{\gamma_{\mathrm{S}} L_{\mathrm{SR}}^{-\alpha}\|\mathbf{h}_{\mathrm{SR}}\|^2, \gamma_{\mathrm{R}} l^{-\alpha}\frac{|\mathbf{h}_{\mathrm{RD}}^T\mathbf{h}_{\mathrm{RE}}^*|^2}{\|\mathbf{h}_{\mathrm{RD}}\|^2}\right\}. \tag{26}$$

Similarly, when only considering the direct S-Ei link, we can infer the instantaneous SNR at Ei from (2), i.e.

$$\widehat{\mathrm{SNR}}_{\mathrm{E,\ direct}}^{DF} = \gamma_{\mathrm{S}} l_{\mathrm{SE}}^{-\alpha}|h_{\mathrm{SE}}|^2. \tag{27}$$

Finally, with the assumption that Ei uses MRC to combine signals from direct and indirect links, the instantaneous SNR at Ei is given by [26]

$$\begin{aligned}\widehat{\mathrm{SNR}}_{\mathrm{E}}^{DF} &= \widehat{\mathrm{SNR}}_{\mathrm{E,\ indirect}}^{DF} + \widehat{\mathrm{SNR}}_{\mathrm{E,\ direct}}^{DF}\\ &= \min\left\{\gamma_{\mathrm{S}} L_{\mathrm{SR}}^{-\alpha}\|\mathbf{h}_{\mathrm{SR}}\|^2, \gamma_{\mathrm{R}} l^{-\alpha}\frac{|\mathbf{h}_{\mathrm{RD}}^T\mathbf{h}_{\mathrm{RE}}^*|^2}{\|\mathbf{h}_{\mathrm{RD}}\|^2}\right\}\\ &\quad + \gamma_{\mathrm{S}} l_{\mathrm{SE}}^{-\alpha}|h_{\mathrm{SE}}|^2.\end{aligned} \tag{28}$$

From (1) and (16), the instantaneous SNR at D can be written as [29]

$$\widehat{\mathrm{SNR}}_{\mathrm{D}}^{DF} = \min\left\{\gamma_{\mathrm{S}} L_{\mathrm{SR}}^{-\alpha}\|\mathbf{h}_{\mathrm{SR}}\|^2, \gamma_{\mathrm{R}} L_{\mathrm{RD}}^{-\alpha}\|\mathbf{h}_{\mathrm{RD}}\|^2\right\}. \tag{29}$$

Observation: From (24)–(25) we can see that both $\widehat{\mathrm{SNR}}_{\mathrm{E}}^{AF}$ and $\widehat{\mathrm{SNR}}_{\mathrm{D}}^{AF}$ are increasing functions of γ_{S}. Thus, there will be a need to determine a suitable value of γ_{S} in making the trade-off between these SNRs. In contrast, the same does not hold for $\widehat{\mathrm{SNR}}_{\mathrm{E}}^{DF}$ and $\widehat{\mathrm{SNR}}_{\mathrm{D}}^{DF}$. In both relaying operations, γ_{R} will not enter into our trade-off problem. With the large number of antennas configured at R, it is reasonable to keep the average total relay power (i.e. γ_{R}) constant such that the consumed power-per-antenna at R is reduced.

III. SNR Approximation for Large Antenna Arrays

In this section, we will evaluate the secure performance of the proposed system under the assumption that the number of transmit and receive antennas at R is very large. Recall the following well-known properties[6]:

- Property (P1): Let $\mathbf{p} \in \mathbb{C}^{N\times 1}$ and $\mathbf{q} \in \mathbb{C}^{N\times 1}$ be complex-valued column vectors whose elements are independent and identically distributed (i.i.d.) random variables with zero means and variances of σ_p^2 and σ_q^2. Then $(1/\sqrt{N})\mathbf{p}^T\mathbf{q} \overset{dist}{\to} \mathcal{CN}\left(0, \sigma_p^2\sigma_q^2\right)$ where $\overset{dist}{\to}$ denotes convergence in distribution as $N \to \infty$.
- Property (P2): With $\mathbf{p}$ and $\mathbf{q}$ as in (P1), we have $\frac{1}{N}\|\mathbf{p}\|^2 \xrightarrow{N\to\infty} \sigma_p^2$ and $\frac{1}{N}\|\mathbf{q}\|^2 \xrightarrow{N\to\infty} \sigma_q^2$ where $\xrightarrow{N\to\infty}$ denotes almost-sure convergence as $N \to \infty$.

[6]These properties are derived from the Lindeberg-Levy theorem and law of large numbers (see [2], [30], [31] and references therein).

To proceed, we first rewrite (24)–(25) as

$$\widehat{\mathrm{SNR}}_{\mathrm{D}}^{AF} = N\frac{\gamma_{\mathrm{S}} L_{\mathrm{SR}}^{-\alpha}\gamma_{\mathrm{R}} L_{\mathrm{RD}}^{-\alpha}\frac{\|\mathbf{h}_{\mathrm{SR}}\|^2}{N}\frac{\|\mathbf{h}_{\mathrm{RD}}\|^2}{N}}{\gamma_{\mathrm{S}} L_{\mathrm{SR}}^{-\alpha}\frac{\|\mathbf{h}_{\mathrm{SR}}\|^2}{N} + \gamma_{\mathrm{R}} L_{\mathrm{RD}}^{-\alpha}\frac{\|\mathbf{h}_{\mathrm{RD}}\|^2}{N} + \frac{1}{N}}, \tag{30}$$

$$\begin{aligned}\widehat{\mathrm{SNR}}_{\mathrm{E}}^{AF} &= \gamma_{\mathrm{S}} l_{\mathrm{SE}}^{-\alpha}|h_{\mathrm{SE}}|^2\\ &\quad + N\frac{\gamma_{\mathrm{S}} L_{\mathrm{SR}}^{-\alpha}\gamma_{\mathrm{R}} l^{-\alpha}\frac{\|\mathbf{h}_{\mathrm{SR}}\|^2}{N}\frac{|\mathbf{h}_{\mathrm{RD}}^T\mathbf{h}_{\mathrm{RE}}^*|^2}{N}}{N\left(\gamma_{\mathrm{S}} L_{\mathrm{SR}}^{-\alpha}\frac{\|\mathbf{h}_{\mathrm{SR}}\|^2}{N} + \frac{1}{N}\right)\frac{\|\mathbf{h}_{\mathrm{RD}}\|^2}{N} + \gamma_{\mathrm{R}} l^{-\alpha}\frac{|\mathbf{h}_{\mathrm{RD}}^T\mathbf{h}_{\mathrm{RE}}^*|^2}{N}}\end{aligned} \tag{31}$$

and (28)–(29) as

$$\widehat{\mathrm{SNR}}_{\mathrm{D}}^{DF} = N\min\left\{\gamma_{\mathrm{S}} L_{\mathrm{SR}}^{-\alpha}\frac{\|\mathbf{h}_{\mathrm{SR}}\|^2}{N}, \gamma_{\mathrm{R}} L_{\mathrm{RD}}^{-\alpha}\frac{\|\mathbf{h}_{\mathrm{RD}}\|^2}{N}\right\}, \tag{32}$$

$$\begin{aligned}\widehat{\mathrm{SNR}}_{\mathrm{E}}^{DF} &= \gamma_{\mathrm{S}} l_{\mathrm{SE}}^{-\alpha}|h_{\mathrm{SE}}|^2\\ &\quad + N\min\left\{\gamma_{\mathrm{S}} L_{\mathrm{SR}}^{-\alpha}\frac{\|\mathbf{h}_{\mathrm{SR}}\|^2}{N}, \gamma_{\mathrm{R}} l^{-\alpha}\frac{|\mathbf{h}_{\mathrm{RD}}^T\mathbf{h}_{\mathrm{RE}}^*|^2}{N}\frac{\frac{1}{N}}{\frac{\|\mathbf{h}_{\mathrm{RD}}\|^2}{N}}\right\}.\end{aligned} \tag{33}$$

Then, respectively applying Property (P1) to the term $\frac{\mathbf{h}_{\mathrm{RD}}^T\mathbf{h}_{\mathrm{RE}}^*}{\sqrt{N}}$ and applying Property (P2) to the terms $\frac{\|\mathbf{h}_{\mathrm{SR}}\|^2}{N}$ and $\frac{\|\mathbf{h}_{\mathrm{RD}}\|^2}{N}$, we can arrive at the following approximate expressions:

$$\widehat{\mathrm{SNR}}_{\mathrm{D}}^{AF} \approx \frac{\gamma_{\mathrm{S}} L_{\mathrm{SR}}^{-\alpha}\gamma_{\mathrm{R}} L_{\mathrm{RD}}^{-\alpha}N^2}{\gamma_{\mathrm{S}} L_{\mathrm{SR}}^{-\alpha}N + \gamma_{\mathrm{R}} L_{\mathrm{RD}}^{-\alpha}N + 1} \triangleq \mathrm{snr}_{\mathrm{D}}^{AF}, \tag{34}$$

$$\begin{aligned}\widehat{\mathrm{SNR}}_{\mathrm{E}}^{AF} &\approx \frac{\gamma_{\mathrm{S}} L_{\mathrm{SR}}^{-\alpha}\gamma_{\mathrm{R}} l^{-\alpha}N\Theta}{\left(\gamma_{\mathrm{S}} L_{\mathrm{SR}}^{-\alpha}N + 1\right) + \gamma_{\mathrm{R}} l^{-\alpha}\Theta} + \gamma_{\mathrm{S}} l_{\mathrm{SE}}^{-\alpha}|h_{\mathrm{SE}}|^2\\ &\triangleq \mathrm{snr}_{\mathrm{E}}^{AF},\end{aligned} \tag{35}$$

$$\widehat{\mathrm{SNR}}_{\mathrm{D}}^{DF} \approx \min\left\{\gamma_{\mathrm{S}} L_{\mathrm{SR}}^{-\alpha}N, \gamma_{\mathrm{R}} L_{\mathrm{RD}}^{-\alpha}N\right\} \triangleq \mathrm{snr}_{\mathrm{D}}^{DF}, \tag{36}$$

$$\begin{aligned}\widehat{\mathrm{SNR}}_{\mathrm{E}}^{DF} &\approx \min\left\{\gamma_{\mathrm{S}} L_{\mathrm{SR}}^{-\alpha}N, \gamma_{\mathrm{R}} l^{-\alpha}\Theta\right\} + \gamma_{\mathrm{S}} l_{\mathrm{SE}}^{-\alpha}|h_{\mathrm{SE}}|^2\\ &\triangleq \mathrm{snr}_{\mathrm{E}}^{DF}\end{aligned} \tag{37}$$

where $\Theta \triangleq \frac{1}{N}\left|\mathbf{h}_{\mathrm{RD}}\mathbf{h}_{\mathrm{RE}}^{\dagger}\right|^2$. Note that we have $\frac{1}{\sqrt{N}}\mathbf{h}_{RD}\mathbf{h}_{RE}^{\dagger} \overset{dist}{\to} \mathcal{CN}(0,1)$ by using Property (P_1) and thus, $\Theta \sim \mathsf{Exp}(1)$.[7] In (34)–(37), $\mathrm{snr}_{\mathrm{D}}^{AF}$, $\mathrm{snr}_{\mathrm{E}}^{AF}$, $\mathrm{snr}_{\mathrm{D}}^{DF}$ and $\mathrm{snr}_{\mathrm{E}}^{DF}$ are functions of N.

Let Emax denote the strongest eavesdropper, i.e., that which receives with the largest instantaneous SNR among all eavesdroppers E$i \in \Psi$. Then the instantaneous SNRs at Emax in the AF scheme ($\widehat{\mathrm{SNR}}_{\mathrm{E}max}^{AF}$) and in the DF scheme ($\widehat{\mathrm{SNR}}_{\mathrm{E}max}^{DF}$) are approximated as

$$\widehat{\mathrm{SNR}}_{\mathrm{E}max}^{AF} \equiv \max_{\mathrm{E}i\in\Psi}\widehat{\mathrm{SNR}}_{\mathrm{E}}^{AF} \approx \max_{\mathrm{E}i\in\Psi}\mathrm{snr}_{\mathrm{E}}^{AF}, \tag{38}$$

$$\widehat{\mathrm{SNR}}_{\mathrm{E}max}^{DF} \equiv \max_{\mathrm{E}i\in\Psi}\widehat{\mathrm{SNR}}_{\mathrm{E}}^{DF} \approx \max_{\mathrm{E}i\in\Psi}\mathrm{snr}_{\mathrm{E}}^{DF}. \tag{39}$$

To facilitate a general analysis that can be applied to both schemes, we use the following notation: $\widehat{\mathrm{SNR}}_{\mathrm{D}} = \left\{\widehat{\mathrm{SNR}}_{\mathrm{D}}^{AF}, \widehat{\mathrm{SNR}}_{\mathrm{D}}^{DF}\right\}$, $\widehat{\mathrm{SNR}}_{\mathrm{E}} = \left\{\widehat{\mathrm{SNR}}_{\mathrm{E}}^{AF}, \widehat{\mathrm{SNR}}_{\mathrm{E}}^{DF}\right\}$, $\mathrm{snr}_{\mathrm{D}} = \left\{\mathrm{snr}_{\mathrm{D}}^{AF}, \mathrm{snr}_{\mathrm{D}}^{DF}\right\}$, $\mathrm{snr}_{\mathrm{E}} = \left\{\mathrm{snr}_{\mathrm{E}}^{AF}, \mathrm{snr}_{\mathrm{E}}^{DF}\right\}$, and $\max_{\mathrm{E}i\in\Psi}\mathrm{snr}_{\mathrm{E}} = \left\{\max_{\mathrm{E}i\in\Psi}\mathrm{snr}_{\mathrm{E}}^{AF}, \max_{\mathrm{E}i\in\Psi}\mathrm{snr}_{\mathrm{E}}^{DF}\right\}$.

[7]$\mathsf{Exp}(r)$ denotes the exponential distribution with rate r. If $z \sim \mathcal{CN}\left(0,\sigma^2\right)$, then $|z|^2 \sim \mathsf{Exp}\left(1/\sigma^2\right)$.

Proposition 1: The cumulative distribution function (CDF) of snr_E^{AF} is given by

$$F_{snr_E^{AF}}(\mu) = 1 - \mathcal{T}_{\mu_m}(l)\mathbb{1}(\mu_m < \gamma_S L_{SR}^{-\alpha} N) - \frac{\gamma_S L_{SR}^{-\alpha} N(1+\gamma_S L_{SR}^{-\alpha} N)}{\gamma_R l^{-\alpha}} \mathcal{J}_{\mu_m}(l, l_{SE}) \quad (40)$$

where

$$\mu_m \triangleq \min\{\mu, \gamma_S L_{SR}^{-\alpha} N\},$$

$$\mathbb{1}(\mathbf{C}) = \begin{cases} 1, & \textit{if } \mathbf{C} \textit{ is true} \\ 0, & \textit{otherwise}, \end{cases} \quad (41)$$

$$\mathcal{T}_{\mu_m}(l) \triangleq \exp\left\{ \frac{(1+\gamma_S L_{SR}^{-\alpha} N)\mu_m}{\gamma_R l^{-\alpha}(\mu_m - \gamma_S L_{SR}^{-\alpha} N)} \right\} \quad (42)$$

and

$$\mathcal{J}_{\mu_m}(l, l_{SE}) \triangleq e^{-\frac{\mu}{\gamma_S l_{SE}^{-\alpha}}} \int_0^{\mu_m} \frac{e^{\frac{x}{\gamma_S l_{SE}^{-\alpha}} + \frac{(1+\gamma_S L_{SR}^{-\alpha} N)x}{\gamma_R l^{-\alpha}(x - \gamma_S L_{SR}^{-\alpha} N)}}}{(x - \gamma_S L_{SR}^{-\alpha} N)^2} dx. \quad (43)$$

Proof: See Appendix A. □

Proposition 2: The CDF of snr_E^{DF} is given by

$$F_{snr_E^{DF}}(\mu) = 1 - e^{-\frac{\mu_m}{\gamma_R l^{-\alpha}}} + \frac{\gamma_S l_{SE}^{-\alpha}}{\gamma_R l^{-\alpha} - \gamma_S l_{SE}^{-\alpha}} e^{-\frac{\mu}{\gamma_S l_{SE}^{-\alpha}}} \times \left[1 - e^{\mu_m \left(\frac{1}{\gamma_S l_{SE}^{-\alpha}} - \frac{1}{\gamma_R l^{-\alpha}} \right)} \right] + e^{-\frac{\gamma_S L_{SR}^{-\alpha} N}{\gamma_R l^{-\alpha}}} \left[1 - e^{-\frac{(\mu - \mu_m)}{\gamma_S l_{SE}^{-\alpha}}} \right] \mathbb{1}(\mu > \gamma_S L_{SR}^{-\alpha} N). \quad (44)$$

Proof: See Appendix B. □

IV. Secrecy Outage Probability (SOP)

In this section, we evaluate the secure performance of the proposed system through the SOP. We first suppose that E*i* succeeds in partially decoding the received signal if its instantaneous SNR is larger than or equal to a certain threshold μ. When eavesdroppers are non-colluding, we can define an *outage event* as the event in which "there is at least one E*i* that can partially decode its received signal." Based on this definition, the SOP is referred to as the probability of the occurrence of the *outage event*, i.e.

$$\widehat{\text{SOP}}_\mu \triangleq \mathbb{P}\{\textit{outage event}\} = \mathbb{P}\left\{ \exists\, \text{E}i \in \Psi \,\middle|\, \widehat{\text{SNR}}_\text{E} \geq \mu \right\} = \mathbb{P}\left\{ \max_{\text{E}i \in \Psi} \widehat{\text{SNR}}_\text{E} \geq \mu \right\} \quad (45)$$

in which $\max_{\text{E}i\in\Psi} \widehat{\text{SNR}}_\text{E} \geq \mu$ implies that among existing eavesdroppers, the eavesdropper with the maximum received SNR can decode signals.[8]

A. Analysis With Large N

Under the assumption of (very) large N, we can use (45), (38) and (39) to arrive at the following approximation:

$$\begin{aligned} \widehat{\text{SOP}}_\mu &\approx \text{SOP}_\mu \\ &= \mathbb{P}\left\{ \max_{\text{E}i\in\Psi} \text{snr}_\text{E} \geq \mu \right\} \\ &= 1 - \mathbb{E}_\Psi \left\{ \prod_{\text{E}i\in\Psi} \mathbb{P}\left\{ \text{snr}_\text{E} < \mu \middle| \Psi \right\} \right\} \\ &\overset{(a)}{=} 1 - \exp\left\{ -\lambda \int_0^{2\pi} \int_0^{R_\Psi} \left(1 - F_{\text{snr}_\text{E}}(\mu)\right) l dl d\phi \right\} \end{aligned} \quad (46)$$

where the equality (a) follows from the application of the *probability generating function* (PGF) [16]. Herein, $\mathbb{P}\{\text{snr}_\text{E} < \mu | \Psi\} = F_{\text{snr}_\text{E}}(\mu)$ is the probability that a given E*i* cannot decode the received signal. In the following, we evaluate the SOP for the two relaying protocols of interest. Denote $\text{SOP}_\mu \equiv \text{SOP}_\mu^{AF}$ and $\text{SOP}_\mu \equiv \text{SOP}_\mu^{DF}$ for the two different relaying cases.

1) AF Scheme: The SOP in the AF case is given by

$$\text{SOP}_\mu^{AF} = 1 - \exp\left\{ -\lambda \int_0^{2\pi} \int_0^{R_\Psi} \underbrace{\left(1 - F_{\text{snr}_\text{E}^{AF}}(\mu)\right)}_{\text{a function of } l \text{ and } \phi} l dl d\phi \right\}. \quad (47)$$

[8]For the colluding eavesdroppers scenario, the outage event should be defined as the event of the occurrence $\sum_{\text{E}i\in\Psi} \widehat{\text{SNR}}_\text{E} \geq \mu$. This interesting scenario might not be mathematically tractable and is a topic for future consideration.

$$\text{SOP}_\mu^{AF} = 1 - \exp\Bigg\{ -\lambda \int_0^{2\pi} \int_0^{R_\Psi} \Bigg[\exp\left\{ \frac{(1+\gamma_\text{S} L_\text{SR}^{-\alpha} N)\mu_m}{\gamma_\text{R} l^{-\alpha}(\mu_m - \gamma_\text{S} L_\text{SR}^{-\alpha} N)} \right\} \mathbb{1}(\mu_m < \gamma_\text{S} L_\text{SR}^{-\alpha} N) + \frac{\gamma_\text{S} L_\text{SR}^{-\alpha} N(1+\gamma_\text{S} L_\text{SR}^{-\alpha} N)}{\gamma_\text{R} l^{-\alpha}} \exp\left\{ \frac{-\mu}{\gamma_\text{S}(L_\text{SR}^2 + l^2 - 2L_\text{SR} l\cos\phi)^{-\alpha/2}} \right\} \times \int_0^{\mu_m} \frac{\exp\left\{ \frac{x}{\gamma_\text{S}(L_\text{SR}^2 + l^2 - 2L_\text{SR} l\cos\phi)^{-\alpha/2}} + \frac{(1+\gamma_\text{S} L_\text{SR}^{-\alpha} N)x}{\gamma_\text{R} l^{-\alpha}(x - \gamma_\text{S} L_\text{SR}^{-\alpha} N)} \right\}}{(x - \gamma_\text{S} L_\text{SR}^{-\alpha} N)^2} dx \Bigg] l dl d\phi \Bigg\} \quad (49)$$

$$\mathrm{SOP}_{\mu}^{DF} = 1 - \exp\Bigg\{-\lambda \int_0^{2\pi}\int_0^{R_\Psi}\Bigg[e^{-\frac{\mu_m}{\gamma_{\mathrm{R}} l^{-\alpha}}} - e^{-\frac{\gamma_{\mathrm{S}} L_{\mathrm{SR}}^{-\alpha} N}{\gamma_{\mathrm{R}} l^{-\alpha}}}\left(1 - e^{\frac{\mu_m - \mu}{\gamma_{\mathrm{S}}\left(L_{\mathrm{SR}}^2 + l^2 - 2L_{\mathrm{SR}} l\cos\phi\right)^{-\alpha/2}}}\right)\mathbb{1}(\mu > \gamma_{\mathrm{S}} L_{\mathrm{SR}}^{-\alpha} N)$$
$$- \frac{\gamma_{\mathrm{S}}\left(L_{\mathrm{SR}}^2 + l^2 - 2L_{\mathrm{SR}} l\cos\phi\right)^{-\alpha/2}}{\gamma_{\mathrm{R}} l^{-\alpha} - \gamma_{\mathrm{S}}\left(L_{\mathrm{SR}}^2 + l^2 - 2L_{\mathrm{SR}} l\cos\phi\right)^{-\alpha/2}} \exp\left\{-\frac{\mu}{\gamma_{\mathrm{S}}\left(L_{\mathrm{SR}}^2 + l^2 - 2L_{\mathrm{SR}} l\cos\phi\right)^{-\alpha/2}}\right\}$$
$$\times\left(1 - \exp\left\{\mu_m\left(\frac{1}{\gamma_{\mathrm{S}}\left(L_{\mathrm{SR}}^2 + l^2 - 2L_{\mathrm{SR}} l\cos\phi\right)^{-\alpha/2}} - \frac{1}{\gamma_{\mathrm{R}} l^{-\alpha}}\right)\right\}\right)\Bigg] l dl d\phi\Bigg\} \tag{55}$$

By substituting (40) into (47), we have

$$\mathrm{SOP}_{\mu}^{AF} = 1 - \exp\Bigg\{-\lambda \int_0^{2\pi}\int_0^{R_\Psi}\Bigg[\mathcal{T}_{\mu_m}(l)\mathbb{1}(\mu_m < \gamma_{\mathrm{S}} L_{\mathrm{SR}}^{-\alpha} N) + \frac{\gamma_{\mathrm{S}} L_{\mathrm{SR}}^{-\alpha} N(1 + \gamma_{\mathrm{S}} L_{\mathrm{SR}}^{-\alpha} N)}{\gamma_{\mathrm{R}} l^{-\alpha}} \mathcal{J}_{\mu_m}(l, l_{\mathrm{SE}})\Bigg] l dl d\phi\Bigg\} \tag{48}$$

which can also be explicitly written as in (49) at the bottom of the previous page.

2) DF Scheme: The SOP in the DF case is given by

$$\mathrm{SOP}_{\mu}^{DF} = 1 - \exp\left\{-\lambda \int_0^{2\pi}\int_0^{R_\Psi} \underbrace{\left(1 - F_{\mathrm{snr}_{\mathrm{E}}^{DF}}(\mu)\right)}_{\text{a function of } l \text{ and } \phi} l dl d\phi\right\} \tag{50}$$

by repeating the same steps as in the derivation of (47). Substituting (44) into the above equation, we arrive at an exact expression for (50) as shown in (55) at the top of this page.

B. Analysis With Large N and High γ_S

With very large N, we proceed to consider the performance at high γ_{S} (i.e. $\gamma_{\mathrm{S}} \to \infty$). With finite μ and large enough N, we have $\mu_m = \min\{\mu, \gamma_{\mathrm{S}} L_{\mathrm{SR}}^{-\alpha} N\} = \mu$. Herein, we do not consider the case of high γ_{R} because the instantaneous increase in N and γ_{R} is obviously costly and impractical. Once N is large, γ_{R} had better be low to reduce the power consumption per antenna at R.

1) AF Scheme: We consider the following terms:

$$\begin{aligned}\mathbb{T}(l) &\triangleq \lim_{\gamma_{\mathrm{S}}\to\infty} \mathcal{T}_{\mu_m}(l)\mathbb{1}\left(\mu_m < \gamma_{\mathrm{S}} L_{\mathrm{SR}}^{-\alpha} N\right) \\ &= \lim_{\gamma_{\mathrm{S}}\to\infty} \exp\left\{\frac{(1 + \gamma_{\mathrm{S}} L_{\mathrm{SR}}^{-\alpha} N)\mu}{\gamma_{\mathrm{R}} l^{-\alpha}(\mu - \gamma_{\mathrm{S}} L_{\mathrm{SR}}^{-\alpha} N)}\right\} \\ &= \exp\left\{-\mu/(\gamma_{\mathrm{R}} l^{-\alpha})\right\}\end{aligned} \tag{51}$$

and

$$\begin{aligned}\mathbb{J}(l) &\triangleq \lim_{\gamma_{\mathrm{S}}\to\infty} \frac{\gamma_{\mathrm{S}} L_{\mathrm{SR}}^{-\alpha} N(1 + \gamma_{\mathrm{S}} L_{\mathrm{SR}}^{-\alpha} N)}{\gamma_{\mathrm{R}} l^{-\alpha}} \mathcal{J}_{\mu_m}(l, l_{\mathrm{SE}}) \\ &= \frac{(\gamma_{\mathrm{S}} L_{\mathrm{SR}}^{-\alpha} N)^2}{\gamma_{\mathrm{R}} l^{-\alpha}} \int_0^{\mu} \frac{e^{\frac{\gamma_{\mathrm{S}} L_{\mathrm{SR}}^{-\alpha} N x}{\gamma_{\mathrm{R}} l^{-\alpha}(-\gamma_{\mathrm{S}} L_{\mathrm{SR}}^{-\alpha} N)}}}{(\gamma_{\mathrm{S}} L_{\mathrm{SR}}^{-\alpha} N)^2} dx \\ &= 1 - \exp\left\{-\mu/(\gamma_{\mathrm{R}} l^{-\alpha})\right\}.\end{aligned} \tag{52}$$

Taking the limit of (40) at $\gamma_{\mathrm{S}} \to \infty$, we have

$$\lim_{\gamma_{\mathrm{S}}\to\infty} F_{\mathrm{snr}_{\mathrm{E}}^{AF}}(\mu) = 1 - \mathbb{T}(l) - \mathbb{J}(l) = 0. \tag{53}$$

Then using the two above-calculated limits, we obtain the limit of $\mathbb{P}\left\{\Lambda_{\mathrm{E}}^{AF}\right\}$ in (48) at $\gamma_{\mathrm{S}} \to \infty$ as follows:

$$\begin{aligned}\mathrm{SOP}_{\mu,asym}^{AF} &= \lim_{\gamma_{\mathrm{S}}\to\infty} \mathrm{SOP}_{\mu}^{AF} \\ &= 1 - \exp\left\{-\lambda \int_0^{2\pi}\int_0^{R_\Psi} (1 - 0)\, l dl d\phi\right\} \\ &= 1 - \exp\left\{-\pi\lambda R_\Psi^2\right\}.\end{aligned} \tag{54}$$

2) DF Scheme: Taking the limit of (44) at $\gamma_{\mathrm{S}} \to \infty$, we have

$$\begin{aligned}\lim_{\gamma_{\mathrm{S}}\to\infty} F_{\mathrm{snr}_{\mathrm{E}}^{DF}}(\mu) &= 1 - e^{-\frac{\mu_m}{\gamma_{\mathrm{R}} l^{-\alpha}}} + \frac{\gamma_{\mathrm{S}} l_{\mathrm{SE}}^{-\alpha}}{\left(-\gamma_{\mathrm{S}} l_{\mathrm{SE}}^{-\alpha}\right)}\left(1 - e^{-\frac{\mu_m}{\gamma_{\mathrm{R}} l^{-\alpha}}}\right) \\ &= 0.\end{aligned} \tag{56}$$

Then, the limit of (50) is given by

$$\begin{aligned}\mathrm{SOP}_{\mu,asym}^{DF} &= \lim_{\gamma_{\mathrm{S}}\to\infty} \mathrm{SOP}_{\mu}^{DF} \\ &= 1 - \exp\left\{-\lambda \int_0^{2\pi}\int_0^{R_\Psi} (1 - 0)\, l dl d\phi\right\} \\ &= 1 - \exp\left\{-\pi\lambda R_\Psi^2\right\}.\end{aligned} \tag{57}$$

Remark 1: We observe from (54) *and* (57) *that when γ_S increases, the role of the considered relaying operations comes to be indistinguishable since both AF and DF give the same value at high γ_S. Indeed, this observation can also be realized in a more intuitive manner: First, we take the limit of* (35)*, i.e,*

$$\begin{aligned}&\lim_{\gamma_S\to\infty} snr_E^{AF} \\ &= \lim_{\gamma_S\to\infty}\left\{\frac{\gamma_S L_{SR}^{-\alpha}\gamma_R l^{-\alpha} N\Theta}{\gamma_S L_{SR}^{-\alpha} N}\right\} + \gamma_S l_{SE}^{-\alpha}|h_{SE}|^2 \\ &= \gamma_R l^{-\alpha}\Theta + \gamma_S l_{SE}^{-\alpha}|h_{SE}|^2, \\ &\lim_{\gamma_S\to\infty} snr_E^{DF} \\ &= \lim_{\gamma_S\to\infty}\left\{\min\left\{\gamma_S L_{SR}^{-\alpha} N, \gamma_R l^{-\alpha}\Theta\right\} + \gamma_S l_{SE}^{-\alpha}|h_{SE}|^2\right\} \\ &= \gamma_R l^{-\alpha}\Theta + \gamma_S l_{SE}^{-\alpha}|h_{SE}|^2.\end{aligned} \tag{58}$$

Then taking the limit of SOP_μ^{AF} in (49) *and SOP_μ^{DF} in* (55)*, we arrive at the same conclusion, i.e.* $\lim_{\gamma_S\to\infty} SOP_\mu^{AF} = \lim_{\gamma_S\to\infty} SOP_\mu^{DF}$.

Proposition 3: For given μ, both SOP_μ^{AF} and SOP_μ^{DF} increase with γ_S. Furthermore, they are upper bounded by the limit $1-\exp\{-\pi\lambda R_\Psi^2\}$, which increases with λ as well as R_Ψ. In this respect, we can conclude that when the eavesdroppers' density λ increases or their working range R_Ψ becomes wider, the upper limit of the SOP in the two relaying cases will increase accordingly.

Proof: Please see Appendix C. □

V. Connection Outage Probability (COP)

To restrict information leakage to a certain extent, we consider an on-off transmission strategy (see, e.g., [32]). As for this strategy, a threshold η is compared to the instantaneous SNR at D before the transmission is performed. More precisely, if $\widehat{\text{SNR}}_\text{D} \leq \eta$, then S keeps silent (OFF-state); otherwise, S will transmit confidential signals (ON-state). As such, the transmission will be in the OFF-state with probability $\mathbb{P}\left\{\widehat{\text{SNR}}_\text{D} \leq \eta\right\}$ which is termed the COP, i.e.

$$\widehat{\text{COP}}_\eta \equiv \mathbb{P}\left\{\text{OFF-state}\right\} \triangleq \mathbb{P}\left\{\widehat{\text{SNR}}_\text{D} \leq \eta\right\}. \tag{59}$$

A. Analysis With Large N

Under the assumption of (very) large N, we can use (59), (34) and (36) to arrive at the following approximation:

$$\widehat{\text{COP}}_\eta \approx \text{COP}_\eta = \mathbb{P}\left\{\text{snr}_\text{D} \leq \eta\right\}. \tag{60}$$

In the following, we analyze the COP for the AF and DF protocols.

1) AF Scheme: We replace snr_D with snr_D^{AF} in the above expression to obtain the COP for the AF case, i.e.

$$\begin{aligned}
\text{COP}_\eta^{AF} &= \mathbb{P}\left\{\text{snr}_\text{D}^{AF} \leq \eta\right\} \\
&= \mathbb{P}\left\{\frac{\gamma_\text{S} L_\text{SR}^{-\alpha}\gamma_\text{R} L_\text{RD}^{-\alpha} N^2}{\gamma_\text{S} L_\text{SR}^{-\alpha} N + \gamma_\text{R} L_\text{RD}^{-\alpha} N + 1} \leq \eta\right\} \\
&= \mathbb{P}\left\{\gamma_\text{S} L_\text{SR}^{-\alpha} N\left(\gamma_\text{R} L_\text{RD}^{-\alpha} N - \eta\right) \leq \eta\left(\gamma_\text{R} L_\text{RD}^{-\alpha} N + 1\right)\right\} \\
&= \begin{cases} 1, & \text{if } \gamma_\text{R} \leq \Omega_\eta \\ \mathbb{P}\left\{\gamma_\text{S} \leq \dfrac{\eta\left(\gamma_\text{R} L_\text{RD}^{-\alpha} N + 1\right)}{L_\text{SR}^{-\alpha} N\left(\gamma_\text{R} L_\text{RD}^{-\alpha} N - \eta\right)}\right\}, & \text{if } \gamma_\text{R} > \Omega_\eta \end{cases} \\
&= \begin{cases} 1, & \text{if } \gamma_\text{R} \leq \Omega_\eta \\ 1, & \text{if } \gamma_\text{R} > \Omega_\eta \text{ and } \gamma_\text{S} \leq \Upsilon_\eta \\ 0, & \text{if } \gamma_\text{R} > \Omega_\eta \text{ and } \gamma_\text{S} > \Upsilon_\eta \end{cases}
\end{aligned} \tag{61}$$

where

$$\Omega_\eta \triangleq \eta / \left(N L_\text{RD}^{-\alpha}\right), \tag{62}$$

$$\Upsilon_\eta \triangleq \frac{\eta\left(\gamma_\text{R} L_\text{RD}^{-\alpha} N + 1\right)}{L_\text{SR}^{-\alpha} L_\text{RD}^{-\alpha} N^2\left(\gamma_\text{R} - \Omega_\eta\right)}. \tag{63}$$

There is no surprise that the COP takes only two values, either 1 or 0, due to the fact that all parameters γ_S, γ_R, N, α, L_SR, L_RD, and η are predetermined. From the design perspective, we want $\text{COP}_\eta = 0$ because it implies that the confidential transmission can occur (in the ON-state). As such, considering the on-off transmission strategy, we must make sure that the two following conditions hold true:

$$\begin{cases} \gamma_\text{R} > \Omega_\eta \\ \gamma_\text{S} > \Upsilon_\eta. \end{cases} \tag{64}$$

2) DF Scheme: With snr_D^{DF} substituted for snr_D in (60), the COP for the DF case can be calculated as

$$\begin{aligned}
\text{COP}_\eta^{DF} &= \mathbb{P}\left\{\text{snr}_\text{D}^{DF} \leq \eta\right\} \\
&= \mathbb{P}\left\{\min\left\{\gamma_\text{S} L_\text{SR}^{-\alpha} N, \gamma_\text{R} L_\text{RD}^{-\alpha} N\right\} \leq \eta\right\} \\
&= \begin{cases} 1, & \text{if } \gamma_\text{S} \leq \omega_\eta \text{ and } \gamma_\text{S} \leq \gamma_\text{R}\left(L_\text{RD}/L_\text{SR}\right)^{-\alpha} \\ 0, & \text{if } \gamma_\text{S} > \omega_\eta \text{ and } \gamma_\text{S} \leq \gamma_\text{R}\left(L_\text{RD}/L_\text{SR}\right)^{-\alpha} \\ 1, & \text{if } \gamma_\text{R} \leq \Omega_\eta \text{ and } \gamma_\text{S} > \gamma_\text{R}\left(L_\text{RD}/L_\text{SR}\right)^{-\alpha} \\ 0, & \text{if } \gamma_\text{R} > \Omega_\eta \text{ and } \gamma_\text{S} > \gamma_\text{R}\left(L_\text{RD}/L_\text{SR}\right)^{-\alpha} \end{cases}
\end{aligned} \tag{65}$$

where

$$\omega_\eta \triangleq \eta / \left(N L_\text{SR}^{-\alpha}\right). \tag{66}$$

Similarly to the AF case, we wish to have $\text{COP}_\eta = 0$, and so

$$\begin{cases} \text{either } \Omega_\eta < \gamma_\text{R} < \gamma_\text{S}\left(L_\text{SR}/L_\text{RD}\right)^{-\alpha} \\ \text{or } \omega_\eta < \gamma_\text{S} \leq \gamma_\text{R}\left(L_\text{RD}/L_\text{SR}\right)^{-\alpha}, \end{cases} \tag{67}$$

needs to be satisfied.

B. Analysis With Large N and High γ_S

As analyzed in the last subsection, we need to set the values of γ_S, γ_R and N such that the COP is equal to 0 for each relaying strategy at R. With high γ_S (i.e. $\gamma_\text{S} \to \infty$) the second condition in (64) is almost surely true, because $\lim_{\gamma_\text{S}\to\infty} \mathbb{P}\left\{\gamma_\text{S} > \Upsilon_\eta\right\} = 1$; thus, the COP in the AF case will approach 0 (i.e. the OFF-state does not occur) at high γ_S given that the first condition in (64) is satisfied. Meanwhile, the second condition in (67) does not seem to be achievable at high γ_S; thus, the COP can reach 0 as long as the first condition in (67) is satisfied. In short, the OFF-state occurs at high γ_S when $\Omega_\eta < \gamma_\text{R}$ for the AF scheme and $\Omega_\eta < \gamma_\text{R} < \gamma_\text{S}\left(L_\text{SR}/L_\text{RD}\right)^{-\alpha}$ for the DF scheme.

VI. Security-Reliability Tradeoff

In this section, we evaluate the interactions of the key secure metrics including the SOP, the COP and the end-to-end (e2e) secrecy rate (SR). In this analysis, the SOP and the COP will be jointly evaluated in another probabilistic metric, i.e. the probability of achieving the most secure transmission state. On letting $\widehat{\mathcal{A}}$ denote the most secure transmission state and $\mathcal{A}$ denote the replacement for $\widehat{\mathcal{A}}$ in the case of (very) large N, we have $\mathbb{P}\{\widehat{\mathcal{A}}\} \approx \mathbb{P}\{\mathcal{A}\}$. Similarly, with large N, the e2e SR (in nats/s/Hz) can be expressed as $C_s = \frac{1}{2}\max\left\{\ln\left(\frac{1+\text{snr}_\text{D}}{1+\text{snr}_{\text{E}max}}\right), 0\right\}$ where the factor of $1/2$ is due to the fact that the transmission is divided into two equal time slots. All metrics C_s, SOP_μ and COP_η involve the same parameter γ_S; thus, we respectively rewrite C_s, SOP_μ and COP_η as $C_s(\gamma_\text{S})$, $\text{SOP}_\mu(\gamma_\text{S})$ and $\text{COP}_\eta(\gamma_\text{S})$ to emphasize the role of γ_S in our analysis.

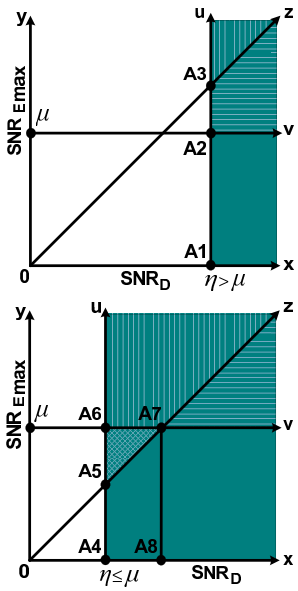

Fig. 2. Possible insecure/secure states of the proposed system versus corresponding ranges of $(\text{snr}_\text{D}, \text{snr}_{\text{E}max})$.

Now, let us look at Fig. 2 which is provided for illustration. In the figure, there are two regions for the e2e SR: the region $y0z$ corresponds to $C_s(\gamma_\text{S}) = 0$ (i.e. $\text{snr}_\text{D} \leq \text{snr}_{\text{E}max}$), while the region $x0z$ corresponds to $C_s(\gamma_\text{S}) > 0$ (i.e. $\text{snr}_\text{D} > \text{snr}_{\text{E}max}$). Further in Fig. 2, we consider two scenarios for η as follows:

- With $\eta > \mu$, the transmission only occurs in the ON-state ($\text{COP}_\eta(\gamma_\text{S}) = 0$) if a pair of $(\text{snr}_\text{D}, \text{snr}_{\text{E}max})$ lies in the region uA_1x. In this case, there are three subcases corresponding to three regions:
  - uA_3z has $C_s(\gamma_\text{S}) = 0$ and $\text{snr}_{\text{E}max} \geq \mu$
  - zA_3A_2v has $C_s(\gamma_\text{S}) > 0$ and $\text{snr}_{\text{E}max} \geq \mu$
  - vA_2A_1x has $C_s(\gamma_\text{S}) > 0$ and $\text{snr}_{\text{E}max} < \mu$
- With $\eta \leq \mu$, the transmission only occurs (in the ON-state) if the considered pair of instantaneous SNRs lies in the region uA_4x. In this case, there are four subcases:
  - uA_6A_7z has $C_s(\gamma_\text{S}) = 0$ and $\text{snr}_{\text{E}max} \geq \mu$
  - zA_7v has $C_s(\gamma_\text{S}) > 0$ and $\text{snr}_{\text{E}max} \geq \mu$
  - $A_5A_6A_7$ has $C_s(\gamma_\text{S}) = 0$ and $\text{snr}_{\text{E}max} < \mu$
  - $vA_7A_5A_4x$ has $C_s(\gamma_\text{S}) > 0$ and $\text{snr}_{\text{E}max} < \mu$

Obviously, if we have $(\text{snr}_\text{D}, \text{snr}_{\text{E}max}) \in vA_2A_1x$ in the case of $\eta > \mu$ and/or $(\text{snr}_\text{D}, \text{snr}_{\text{E}max}) \in vA_7A_5A_4x$ in the case of $\eta \leq \mu$, the proposed system will attain the most secure state with $C_s(\gamma_\text{S}) > 0$, $\text{COP}_\mu(\gamma_\text{S}) = 0$ and $\text{snr}_{\text{E}max} < \mu$. We focus only on the case of $\eta > \mu$ in this paper and evaluate the probability of the event $\mathcal{A} = \{(\text{snr}_\text{D}, \text{snr}_{\text{E}max}) \in vA_2A_1x\}$. The probability of the occurrence of the event $\mathcal{A}$ is given by

$$\begin{aligned}\mathbb{P}\{\mathcal{A}\} &= \mathbb{P}\{(\text{snr}_\text{D}, \text{snr}_{\text{E}max}) \in vA_2A_1x \,|\eta > \mu\} \\ &= \mathbb{P}\{\eta < \text{snr}_\text{D}, \text{snr}_{\text{E}max} < \mu\} \\ &= \mathbb{P}\left\{\max_{\text{E}i \in \Psi} \text{snr}_\text{E} < \mu\right\} \mathbb{P}\{\eta < \text{snr}_\text{D}\} \\ &= \left[1 - \text{SOP}_\mu(\gamma_\text{S})\right]\left[1 - \text{COP}_\eta(\gamma_\text{S})\right]. \end{aligned} \tag{68}$$

We will denote $\mathbb{P}\{\mathcal{A}\}$ as $\mathbb{P}\{\mathcal{A}\}^{AF}$ and $\mathbb{P}\{\mathcal{A}\}^{DF}$ for the AF case and DF case, respectively.

A. AF Case

In order to maximize the probability $\mathbb{P}\{\mathcal{A}\}^{AF}$, we aim to solve the following optimization problem:

$$\begin{aligned}(\mathbf{P}^{AF}) \quad &\underset{\gamma_\text{S}}{\text{minimize}}\ \text{SOP}_\mu^{AF}(\gamma_\text{S}) \\ &\text{subject to } \text{COP}_\eta^{AF}(\gamma_\text{S}) = 0.\end{aligned}$$

Using (64), the constraints are $\gamma_\text{R} > \Omega_\eta$ and $\gamma_\text{S} > \Upsilon_\eta$. Once the constraint $\gamma_\text{R} > \Omega_\eta$ is satisfied, $(\mathbf{P}^{AF})$ has the optimal solution

$$\gamma_{\text{S},opt} \to \Upsilon_\eta^+ \tag{69}$$

because $\text{SOP}_\mu^{AF}(\gamma_\text{S}) > \text{SOP}_\mu^{AF}(\Upsilon_\eta)$ for all $\gamma_\text{S} > \Upsilon_\eta$ (according to Proposition 3). In contrast, if the constraint $\gamma_\text{R} > \Omega_\eta$ is not satisfied, the event $\mathcal{A}$ does not occur regardless of any value of γ_S. As such, we have

$$\max_{\gamma_\text{S}} \mathbb{P}\{\mathcal{A}\}^{AF} = \begin{cases} 1 - \text{SOP}_\mu^{AF}(\Upsilon_\eta^+), & \text{if } \gamma_\text{R} > \Omega_\eta \\ 0, & \text{if } \gamma_\text{R} \leq \Omega_\eta. \end{cases} \tag{70}$$

B. DF Case

Analogously to the AF case, we suggest the optimization problem for the DF case as follows:

$$\begin{aligned}(\mathbf{P}^{DF}) \quad &\underset{\gamma_\text{S}}{\text{minimize}}\ \text{SOP}_\mu^{DF}(\gamma_\text{S}) \\ &\text{subject to } \text{COP}_\eta^{DF}(\gamma_\text{S}) = 0.\end{aligned}$$

Using (67), the constraint becomes $\Omega_\eta < \gamma_\text{R} < \gamma_\text{S}\,(L_{\text{SR}}/L_{\text{RD}})^{-\alpha}$ or $\omega_\eta < \gamma_\text{S} \leq \gamma_\text{R}\,(L_{\text{RD}}/L_{\text{SR}})^{-\alpha}$. Moreover, $\text{SOP}_\mu(\gamma_\text{S})$ increases with γ_S, and so the problem $(\mathbf{P}^{DF})$ has two optimal solutions:

$$\begin{aligned}&\gamma_{\text{S},opt} \\ &= \begin{cases} \gamma_\text{R}^+\,(L_{\text{RD}}/L_{\text{SR}})^{-\alpha}, & \text{if } \gamma_\text{R} > \Omega_\eta \\ \omega_\eta^+, & \text{if } \gamma_\text{R} \geq \omega_\eta^+\,(L_{\text{SR}}/L_{\text{RD}})^{-\alpha} \triangleq \varpi. \end{cases}\end{aligned} \tag{71}$$

Finally, the maximal value of $\mathbb{P}\{\mathcal{A}\}^{DF}$ can be readily deduced from (71) as follows:

$$\begin{aligned}&\max_{\gamma_\text{S}} \mathbb{P}\{\mathcal{A}\}^{DF} \\ &= \begin{cases} \max\left\{\mathbb{P}\{\mathcal{A}\}_{opt,1}^{DF}, \mathbb{P}\{\mathcal{A}\}_{opt,1}^{DF}\right\}, & \text{if } \Omega_\eta < \varpi \leq \gamma_\text{R} \\ & \quad \text{or } \gamma_\text{R} > \Omega_\eta \geq \varpi, \\ \mathbb{P}\{\mathcal{A}\}_{opt,1}^{DF}, & \text{if } \Omega_\eta < \gamma_\text{R} < \varpi, \\ \mathbb{P}\{\mathcal{A}\}_{opt,2}^{DF}, & \text{if } \Omega_\eta \geq \gamma_\text{R} \geq \varpi, \\ 0, & \text{if } \gamma_\text{R} \leq \Omega_\eta < \varpi \\ & \quad \text{or } \Omega_\eta \geq \varpi > \gamma_\text{R} \end{cases}\end{aligned} \tag{72}$$

where $\mathbb{P}\{\mathcal{A}\}_{opt,1}^{DF} \triangleq 1 - \text{SOP}_\mu^{DF}(\gamma_\text{S})\Big|_{\gamma_\text{S}=\omega_\eta^+}$ and $\mathbb{P}\{\mathcal{A}\}_{opt,2}^{DF} \triangleq 1 - \text{SOP}_\mu^{DF}(\gamma_\text{S})\Big|_{\gamma_\text{S}=\gamma_\text{R}^+(L_{\text{RD}}/L_{\text{SR}})^{-\alpha}}$.

Remark 2: Both cases require cooperation between S and R such that γ_S and γ_R meet the requirement for quality of service

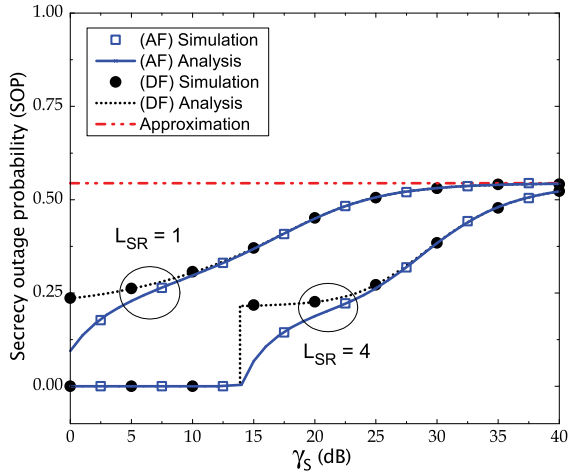

Fig. 3. SOP_{μ}^{AF} in (49) and SOP_{μ}^{DF} in (55) versus γ_{S}. For each relaying scheme, two subcases are considered: $L_{\mathrm{SR}} = 1$ and $L_{\mathrm{SR}} = 4$. Other parameters: $N = 50$, $\lambda = 0.25$, $R_{\Psi} = 1$, $\alpha = 2.5$, $\gamma_{\mathrm{R}} = 10$ dB, $\mu = 16.02$ dB.

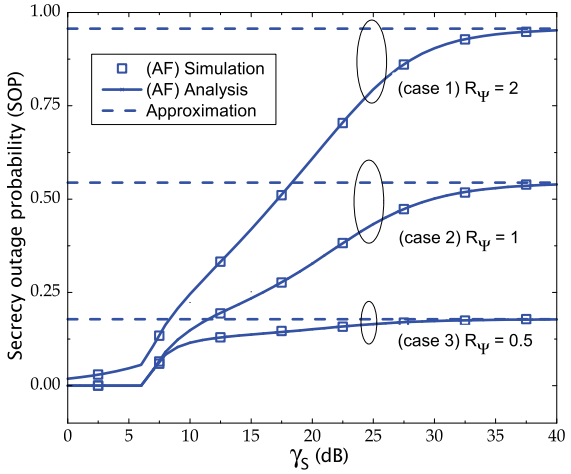

Fig. 4. SOP_{μ}^{AF} in (49) versus γ_{S}. For each relaying scheme, two subcases are considered: (case 1) $R_{\Psi} = 2$; (case 2) $R_{\Psi} = 1$; and (case 3) $R_{\Psi} = 0.5$. Other parameters: $N = 50$, $\lambda = 0.25$, $L_{\mathrm{SR}} = 2$, $\alpha = 2.5$, $\gamma_{\mathrm{R}} = 10$ dB, $\mu = 16.02$ dB.

(i.e. $\mathbb{P}\{\mathcal{A}\}$ is maximized). When the parameter γ_R is chosen beforehand, we only need to set the parameter γ_S to reach the goal. Hence, we choose $\gamma_R > \Omega_\eta$ in the AF case, while, γ_R should satisfy either $\Omega_\eta < \varpi \leq \gamma_R$ or $\gamma_R > \Omega_\eta \geq \varpi$ in the DF case.

VII. Numerical Results

This section provides several numerical examples to verify the correctness of our analysis and show secure characteristics of the proposed system. Relating to distance parameters, the distance reference R_0 is traditionally selected from 100 m to 1 km for large cellular systems [22]–[24]. With the selection of R_0 within $[100m, 1000m]$, the measurement unit of λ will be implicitly understood as the average number of eavesdroppers over $R_0 \times R_0$ m^2. Note that the selected value of R_0 does not change our numerical results, which depend on the distance ratios L_{SR}, L_{RD} and R_{Ψ}. Furthermore, a suitable value of the path loss exponent α should be from 2 to 3. Thus, we choose to set $\alpha = 2.5$ for all numerical examples. Finally, we note that all simulation results have been performed for $\widehat{\mathrm{SOP}}_{\mu}$, $\widehat{\mathrm{COP}}_{\eta}$ and $\mathbb{P}\{\widehat{\mathcal{A}}\}$; whereas, all analytical results have been performed for SOP_{μ}, COP_{η} and $\mathbb{P}\{\mathcal{A}\}$.

In Figs. 3–5, we present the SOPs versus γ_{S} for the AF and DF schemes. The analytical expressions for the SOP are verified through simulation, i.e. $\widehat{\mathrm{SOP}}_{\mu} \approx \mathrm{SOP}_{\mu}$ and $\widehat{\mathrm{SOP}}_{\mu} \approx \mathrm{SOP}_{\mu,asym}$ are confirmed. As seen from the figures, the simulated values of $\widehat{\mathrm{SOP}}_{\mu}$ and the analytical values of SOP_{μ} match each other at large N (i.e. $N = 50$) through the range $[0, 40]$ dB of γ_{S}. Moreover, these values increase with γ_{S} and converges to $\mathrm{SOP}_{\mu,asym}$ at high γ_{S} (for example, at 40 dB).

In Fig. 3, two subcases of L_{SR} are considered, i.e. $L_{\mathrm{SR}} = \{1, 4\}$. We can see that the security performance in the AF case is better than in the DF case for each considered value of L_{SR}. However, when γ_{S} exceeds 15 dB for the case of $L_{\mathrm{SR}} = 1$, the security performance of both schemes is the same and thereby, the role of the relaying protocol becomes indistinguishable.

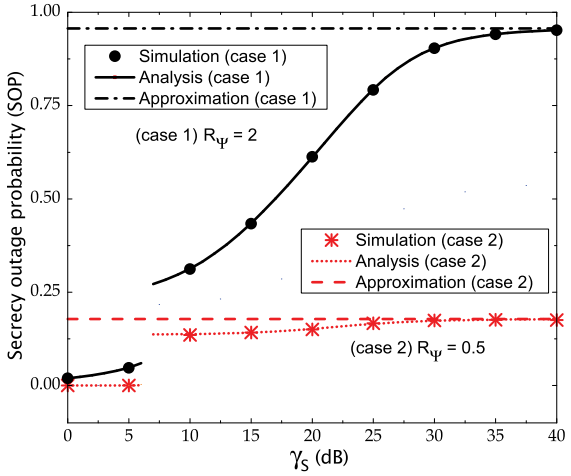

Fig. 5. SOP_{μ}^{DF} in (55) versus γ_{S}. For each relaying scheme, two subcases are considered: (case 1) $R_{\Psi} = 2$; (case 2) $R_{\Psi} = 0.5$. Other parameters: $N = 50$, $\lambda = 0.25$, $L_{\mathrm{SR}} = 2$, $\alpha = 2.5$, $\gamma_{\mathrm{R}} = 10$ dB, $\mu = 16.02$ dB.

Interestingly, the decrease in L_{SR} (i.e. S comes closer to R) does not ensure that the secure performance will be improved.

Regarding Figs. 4–5, we fix the distance ratio L_{SR} and change the radius ratio R_{Ψ}. We observe that the secure performance inversely decreases with the increase in R_{Ψ}. This observation is consistent with the phenomenon that as the working range increases, the eavesdroppers will become more dangerous. In Fig. 6, we depict the SOPs versus λ. Again, the results confirm that the AF scheme gives better secure performance. Moreover, the difference in performance between the two schemes decreases with increasing γ_{S}. Furthermore, an increasing density of eavesdroppers also causes a worse situation for the proposed system (as can be observed intuitively).

In Fig. 7, we depict the COPs versus γ_{S} in the AF case and verify $\widehat{\mathrm{COP}}_{\mu}^{AF} \approx \mathrm{COP}_{\mu}^{AF}$. These results show that when N increases, our analysis becomes smaller because the gap between the simulation curve (i.e. $\widehat{\mathrm{COP}}_{\eta}^{AF}$) and the analytical curve (i.e. COP_{η}^{AF}) is narrowed. In the case

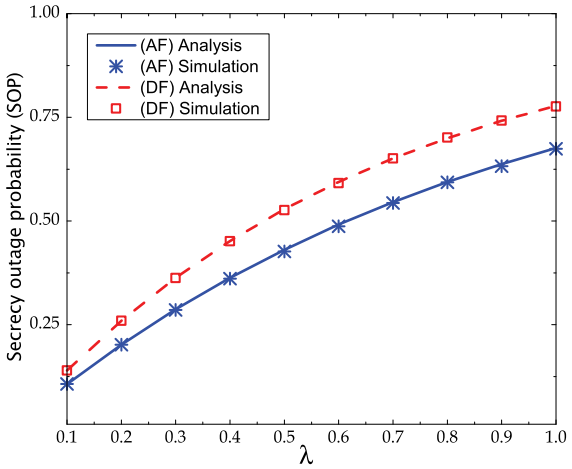

Fig. 6. SOP_{μ}^{AF} in (49) and SOP_{μ}^{DF} in (55) versus λ. Parameters: $N = 50$, $R\Psi = 2$, $L_{\text{SR}} = 2$, $\alpha = 2.5$, $\gamma_{\text{S}} = 10$ dB, $\gamma_{\text{R}} = 10$ dB, $\mu = 16.02$ dB.

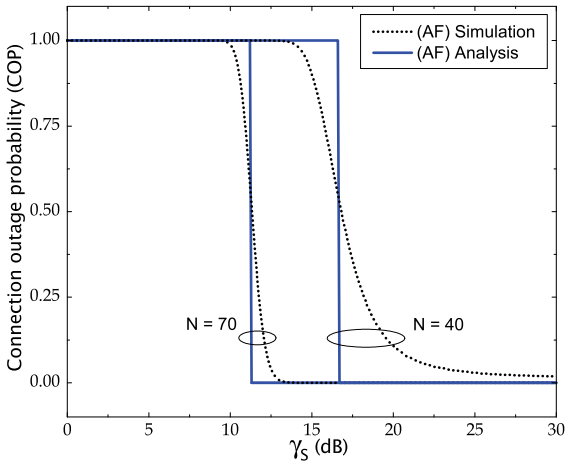

Fig. 7. COP_{η}^{AF} versus γ_{S}. Parameters: $N = \{40, 70\}$, $L_{\text{SR}} = 2$, $L_{\text{RD}} = 1.5$, $\alpha = 2.5$, $\gamma_{\text{R}} = 10$ dB, $\eta = 20$ dB.

of $N = 40$, the first constraint $\gamma_{\text{R}} > \Omega_{\eta}$ is satisfied, i.e. $\gamma_{\text{R}} = 10$ dB > 8.38 dB, and so the COP theoretically reaches 0 at any $\gamma_{\text{R}} > \Upsilon_{\eta} \approx 16.6$ dB. Likewise, in the case of $N = 70$, the constraint $\gamma_{\text{R}} \approx 13.01$ dB > 5.95 dB, and so the COP is expected to be 0 at any $\gamma_{\text{R}} > \Upsilon_{\eta} \approx 11.26$ dB. In comparison between the two cases, we can see that an increase in N helps to enhance the reliability. For example, if the secure transmission occurs at $\gamma_{\text{S}} = 15$ dB, then $N = 70$ will be selected because the theoretical COP equals 0; in contrast, $N = 40$ will lead to an unsecured transmission as the theoretical SOP is 1.

In Fig. 8, we depict the COPs versus γ_{S} in the DF case. Similar to the AF case, the gap between the analysis and simulation becomes smaller when N increases. Moreover, if one of the two conditions in (67) is satisfied, the COP reaches 0. For example, in the case of $N = 40$, the condition $\Omega_{\eta} \approx 10^{8.38/10} < \gamma_{\text{R}} = 10^{10/10}$ dB $< \gamma_{\text{S}}\,(2/1.5)^{-2.5}$ can be attained if $\gamma_{\text{S}} > 13.12$ dB. In the case $N = 70$, the condition $\omega_{\eta} \approx 10^{9.07/10} < \gamma_{\text{S}} \leq 10^{10/10}\,(1.5/2)^{-2.5} \Leftrightarrow 9.07$ dB $< \gamma_{\text{S}} \leq 13.12$ dB will lead to $\text{COP}_{\eta}^{DF} = 0$.

In Fig. 9, the probability of the most secure state $\mathbb{P}\{\mathcal{A}\}^{AF}$ is shown with respect to γ_{S}. The results show that excellent agreement between the analytical curves and the simulation

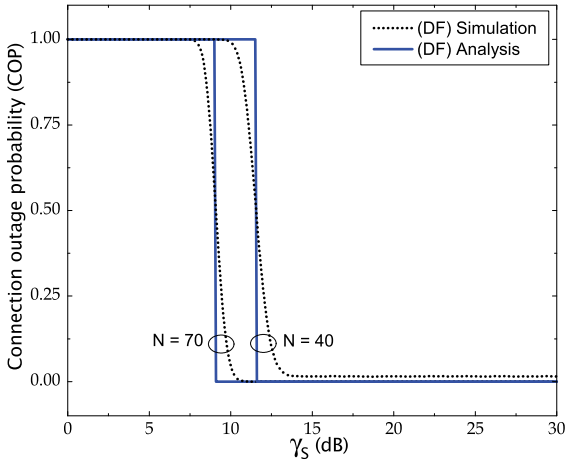

Fig. 8. COP_{η}^{DF} versus γ_{S}. Parameters: $N = \{40, 70\}$, $L_{\text{SR}} = 2$, $L_{\text{RD}} = 1.5$, $\alpha = 2.5$, $\gamma_{\text{R}} = 10$ dB, $\eta = 20$ dB.

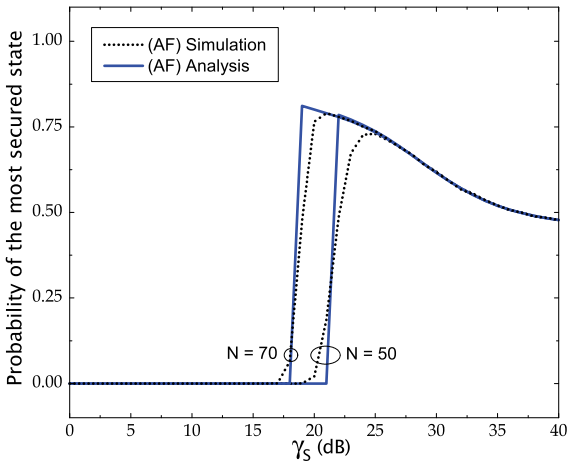

Fig. 9. $\mathbb{P}\{\mathcal{A}\}^{AF}$ versus γ_{S}. Parameters: $N = \{50, 70\}$, $\lambda = 0.25$, $R\Psi = 1$, $L_{\text{SR}} = 4$, $L_{\text{RD}} = 1.5$, $\alpha = 2.5$, $\mu = 16.02$ dB, $\eta = 20$ dB, $\gamma_{\text{R}} = 10$ dB.

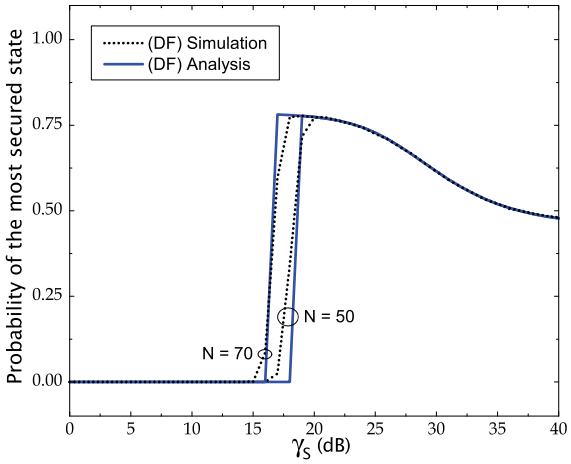

Fig. 10. $\mathbb{P}\{\mathcal{A}\}^{DF}$ versus γ_{S}. Parameters: $N = \{50, 70\}$, $\lambda = 0.25$, $R\Psi = 1$, $L_{\text{SR}} = 4$, $L_{\text{RD}} = 1.5$, $\alpha = 2.5$, $\mu = 16.02$ dB, $\eta = 20$ dB, $\gamma_{\text{R}} = 10$ dB.

curves is attained as N increases. We can see that with $N = 50$, we have $\mathbb{P}\{\mathcal{A}\}^{AF} > 0$ at any $\gamma_{\text{S}} > 21$ dB. In contrast, to have $\mathbb{P}\{\mathcal{A}\}^{AF} > 0$ in the case of $N = 70$, we have to set $\gamma_{\text{S}} > 19$ dB. As such, an increase in N helps ensure $\mathbb{P}\{\mathcal{A}\}^{AF} > 0$ when γ_{S} decreases. As analyzed in Section VI,

$\mathbb{P}\{\mathcal{A}\}^{AF}$ reaches its maximum when $\gamma_S \to \Upsilon_\eta^+$. For example, with $N = 70$ we have $\max_{\gamma_S} \mathbb{P}\{\mathcal{A}\}^{AF} = \mathbb{P}\{\mathcal{A}\}^{AF}\big|_{\gamma_S=\Upsilon_\eta+\epsilon} \approx 0.811$ where ϵ is a very small positive number. Likewise, in Fig. 10, the probability of the most secure state $\mathbb{P}\{\mathcal{A}\}^{DF}$ is also illustrated vs. γ_S. The behavior of $\mathbb{P}\{\mathcal{A}\}^{DF}$ is similar to that of $\mathbb{P}\{\mathcal{A}\}^{AF}$.

VIII. Conclusions

In this paper, we have considered a relay-aided wireless system in which the relay is equipped with a large antenna array in the presence of many potential eavesdroppers, whose positions follow a homogeneous PPP. Furthermore, compared to the destination, the eavesdroppers have the advantage of direct links between them and the source. Under these assumptions, we have employed an ON-OFF strategy and evaluated the security as well as the reliability of the system through probabilistic metrics. Analytical and simulation results show that an increase in the gain γ_S reduces the secure performance in both AF and DF case. Such an increase in γ_S, however, helps enhance the reliability in both AF and DF cases. Finally, optimization problems have been proposed for each relaying scheme such that the probability of achieving the most secure state in each transmission is maximized. Among other conclusions, we have seen that a large value of the array size N makes the COP reach 0, which means that secure transmission can occur for sufficiently large arrays.

Appendix

A. The CDF of snr_E^{AF}

Let us define $\mathcal{X} = \frac{\gamma_S L_{SR}^{-\alpha}\gamma_R l^{-\alpha} N\Theta}{(\gamma_S L_{SR}^{-\alpha} N+1)+\gamma_R l^{-\alpha}\Theta}$. The CDF and probability density function (PDF) of $\mathcal{X}$ can be, respectively, written as

$$\begin{aligned} F_{\mathcal{X}}(x) &= \mathbb{P}\left\{(\gamma_S L_{SR}^{-\alpha} N - x)\gamma_R l^{-\alpha}\Theta \le (\gamma_S L_{SR}^{-\alpha} N + 1)x\right\} \\ &= 1 - \exp\left\{\frac{(1+\gamma_S L_{SR}^{-\alpha} N)x}{\gamma_R l^{-\alpha}(x - \gamma_S L_{SR}^{-\alpha} N)}\right\} \mathbb{1}(x < \gamma_S L_{SR}^{-\alpha} N) \end{aligned} \tag{73}$$

and

$$\begin{aligned} f_{\mathcal{X}}(x) = \exp&\left\{\frac{(1+\gamma_S L_{SR}^{-\alpha} N)x}{\gamma_R l^{-\alpha}(x - \gamma_S L_{SR}^{-\alpha} N)}\right\} \\ &\times \frac{\gamma_S L_{SR}^{-\alpha} N(1+\gamma_S L_{SR}^{-\alpha} N)}{\gamma_R l^{-\alpha}(x - \gamma_S L_{SR}^{-\alpha} N)^2} \mathbb{1}(x < \gamma_S L_{SR}^{-\alpha} N). \end{aligned} \tag{74}$$

As such, snr_E^{AF} in (35) can be rewritten as $\text{snr}_E^{AF} = \gamma_S l_{SE}^{-\alpha}|h_{SE}|^2 + \mathcal{X}$. The CDF of snr_E^{AF} is given by

$$F_{\text{snr}_E^{AF}}(\mu) = \int_0^{\mu_m} F_{|h_{SE}|^2}\left(\frac{\mu - x}{\gamma_S l_{SE}^{-\alpha}}\right) f_{\mathcal{X}}(x)dx \tag{75}$$

where $\mu_m \triangleq \min\{\mu, \gamma_S L_{SR}^{-\alpha} N\}$. After some manipulations, (75) can be expressed in the form of (40).

B. The CDF of snr_E^{DF}

Let us define $\mathcal{Y} = \min\left\{\gamma_S L_{SR}^{-\alpha} N, \gamma_R l^{-\alpha}\Theta\right\}$. The CDF and PDF of $\mathcal{Y}$ can be, respectively, written as

$$F_{\mathcal{Y}}(y) = 1 - \exp\left\{-\frac{y}{\gamma_R l^{-\alpha}}\right\} \mathbb{1}(y < \gamma_S L_{SR}^{-\alpha} N). \tag{76}$$

and

$$\begin{aligned} f_{\mathcal{Y}}(y) = &\frac{1}{\gamma_R l^{-\alpha}} \exp\left\{-\frac{y}{\gamma_R l^{-\alpha}}\right\} \\ &+ \exp\left\{-\frac{\gamma_S L_{SR}^{-\alpha} N}{\gamma_R l^{-\alpha}}\right\} \delta\left(y - \gamma_S L_{SR}^{-\alpha} N\right) \end{aligned} \tag{77}$$

for $y \le \gamma_S L_{SR}^{-\alpha} N$, where $\delta\left(y - \gamma_S L_{SR}^{-\alpha} N\right)$ is a Dirac delta function.

Now we can rewrite snr_E^{DF} in (37) as $\text{snr}_E^{AF} = \gamma_S l_{SE}^{-\alpha}|h_{SE}|^2 + \mathcal{Y}$. The CDF of snr_E^{DF} is given by

$$F_{\text{snr}_E^{DF}}(\mu) = \int_0^{\mu_m} F_{|h_{SE}|^2}\left(\frac{\mu - y}{\gamma_S l_{SE}^{-\alpha}}\right) f_{\mathcal{Y}}(y)dy. \tag{78}$$

After some manipulations, (78) can be expressed in the form of (44).

C. Proof of Proposition 3

First, we note that both snr_E and SOP_μ are functions of γ_S. To emphasize this, we rewrite snr_E and SOP_μ as $\text{snr}_E(\gamma_S)$ and $\text{SOP}_\mu(\gamma_S)$, respectively. It is straightforward to show $\text{snr}_E(p_2) - \text{snr}_E(p_1) \ge 0$ for $p_2 > p_1$, and thus $\text{snr}_E(\gamma_S)$ is an increasing function of γ_S. For $p_2 > p_1$, we have

$$\begin{aligned} &\mathbb{P}\{\text{snr}_E(p_2) < \mu|\Psi\} \\ &\quad < \mathbb{P}\{\text{snr}_E(p_1) < \mu|\Psi\} \\ &\quad \Rightarrow \underbrace{1 - \mathbb{E}_\Psi\left\{\prod_{Ei\in\Psi} \mathbb{P}\{\text{snr}_E(p_2) < \mu|\Psi\}\right\}}_{\text{SOP}_\mu(p_2)} \\ &\quad > \underbrace{1 - \mathbb{E}_\Psi\left\{\prod_{Ei\in\Psi} \mathbb{P}\{\text{snr}_E(p_1) < z|\Psi\}\right\}}_{\text{SOP}_\mu(p_1)} \end{aligned} \tag{79}$$

which demonstrates that $\text{SOP}_\mu(\gamma_S)$ increases with γ_S. Moreover, $\lim_{\gamma_S\to\infty} \text{SOP}_\mu = 1 - \exp\{-\pi\lambda R_\Psi^2\}$ as calculated in (54) and (57) for each considered case; thus this limit value is also an upper bound on SOP_μ at high γ_S.

References

[1] L. J. Rodriguez, N. H. Tran, T. Q. Duong, T. Le-Ngoc, M. Elkashlan, and S. Shetty, "Physical layer security in wireless cooperative relay networks: State of the art and beyond," *IEEE Commun. Mag.*, vol. 53, no. 12, pp. 32–39, Dec. 2015.

[2] F. Rusek *et al.*, "Scaling up MIMO: Opportunities and challenges with very large arrays," *IEEE Signal Process. Mag.*, vol. 30, no. 1, pp. 40–60, Jan. 2013.

[3] X. Chen, J. Chen, and T. Liu, "Secure transmission in wireless powered massive MIMO relaying systems: Performance analysis and optimization," *IEEE Trans. Veh. Technol.*, vol. 64, no. 10, pp. 8025–8035, Oct. 2016.

[4] X. Chen, L. Lei, H. Zhang, and C. Yuen, "Large-scale MIMO relaying techniques for physical layer security: AF or DF?" *IEEE Trans. Wireless Commun.*, vol. 14, no. 9, pp. 5135–5146, Sep. 2015.

[5] G. Amarasuriya, R. F. Schaefer, and H. V. Poor, "Secure communication in massive MIMO relay networks," in *Proc. 17th IEEE Int. Workshop Signal Process. Adv. Wireless Commun. (SPAWC)*, Edinburgh, U.K., Jul. 2016, pp. 1–5.

[6] C. Zhang, J. Ge, J. Li, F. Gong, and H. Ding, "Complexity-aware relay selection for 5G large-scale secure two-way relay systems," *IEEE Trans. Veh. Technol.*, vol. 66, no. 6, pp. 5461–5465, Jun. 2017.

[7] J. Chen, X. Chen, W. H. Gerstacker, and D. W. K. Ng, "Resource allocation for a massive MIMO relay aided secure communication," *IEEE Trans. Inf. Forensics Security*, vol. 11, no. 8, pp. 1700–1711, Aug. 2016.

[8] T. M. Hoang, T. Q. Duong, H. A. Suraweera, C. Tellambura, and H. V. Poor, "Cooperative beamforming and user selection for improving the security of relay-aided systems," *IEEE Trans. Commun.*, vol. 63, no. 12, pp. 5039–5051, Dec. 2015.

[9] J. Zhu and W. Xu, "Securing massive MIMO via power scaling," *IEEE Commun. Lett.*, vol. 20, no. 5, pp. 1014–1017, May 2016.

[10] Y. Wu, R. Schober, D. W. K. Ng, C. Xiao, and G. Caire, "Secure massive MIMO transmission with an active eavesdropper," *IEEE Trans. Inf. Theory*, vol. 62, no. 7, pp. 3880–3900, Jul. 2016.

[11] J. Zhu, D. W. K. Ng, and V. K. Bhargava, "Analysis and design of secure massive MIMO systems in the presence of hardware impairments," *IEEE Trans. Wireless Commun.*, vol. 16, no. 3, pp. 2001–2016, Mar. 2017.

[12] D. Kapetanovic, G. Zheng, and F. Rusek, "Physical layer security for massive MIMO: An overview on passive eavesdropping and active attacks," *IEEE Commun. Mag.*, vol. 53, no. 6, pp. 21–27, Jun. 2015.

[13] C. Wang and H.-M. Wang, "Physical layer security in millimeter wave cellular networks," *IEEE Trans. Wireless Commun.*, vol. 15, no. 8, pp. 5569–5585, Aug. 2016.

[14] H.-M. Wang, C. Wang, T.-X. Zheng, and T. Q. S. Quek, "Impact of artificial noise on cellular networks: A stochastic geometry approach," *IEEE Trans. Wireless Commun.*, vol. 15, no. 11, pp. 7390–7404, Nov. 2016.

[15] S. H. Chae, W. Choi, J. H. Lee, and T. Q. S. Quek, "Enhanced secrecy in stochastic wireless networks: Artificial noise with secrecy protected zone," *IEEE Trans. Inf. Forensics Security*, vol. 9, no. 10, pp. 1617–1628, Oct. 2014.

[16] J. F. C. Kingman, *Poisson Processes*. London, U.K.: Oxford Univ. Press, 1993.

[17] S. N. Chiu, D. Stoyan, W. S. Kendall, and J. Mecke, *Stochastic Geometry and Its Applications*, 3rd ed. New York, NY, USA: Wiley, 2013.

[18] H. Elsawy, E. Hossain, and M. Haenggi, "Stochastic geometry for modeling, analysis, and design of multi-tier and cognitive cellular wireless networks: A survey," *IEEE Commun. Surveys Tuts.*, vol. 15, no. 3, pp. 996–1019, 3rd Quart., 2013.

[19] T. Q. Duong, T. M. Hoang, C. Kundu, M. Elkashlan, and A. Nallanathan, "Optimal power allocation for multiuser secure communication in cooperative relaying networks," *IEEE Wireless Commun. Lett.*, vol. 5, no. 5, pp. 516–519, Oct. 2016.

[20] J. Wang, J. Lee, F. Wang, and T. Q. S. Quek, "Jamming-aided secure communication in massive MIMO Rician channels," *IEEE Trans. Wireless Commun.*, vol. 14, no. 12, pp. 6854–6868, Dec. 2015.

[21] S. M. Azimi-Abarghouyi, M. Nasiri-Kenari, B. Maham, and M. Hejazi, "Integer forcing-and-forward transceiver design for MIMO multipair two-way relaying," *IEEE Trans. Veh. Technol.*, vol. 65, no. 11, pp. 8865–8877, Nov. 2016.

[22] S. Y. Seidel, T. S. Rappaport, S. Jain, M. L. Lord, and R. Singh, "Path loss, scattering, and multipath delay statistics in four European cities for digital cellular and microcellular radiotelephone," *IEEE Trans. Veh. Technol.*, vol. 40, no. 4, pp. 721–730, Nov. 1991.

[23] M. J. Feuerstein, K. L. Blackard, T. S. Rappaport, S. Y. Seidel, and H. Xia, "Path loss, delay spread, and outage models as functions of antenna height for microcellular system design," *IEEE Trans. Veh. Technol.*, vol. 43, no. 3, pp. 487–498, Aug. 1994.

[24] B. Sklar, "Rayleigh fading channels in mobile digital communication systems. I. Characterization," *IEEE Commun. Mag.*, vol. 35, no. 2, pp. 136–146, Sep. 1997.

[25] L. Dong, Z. Han, A. P. Petropulu, and H. V. Poor, "Improving wireless physical layer security via cooperating relays," *IEEE Trans. Signal Process.*, vol. 58, no. 3, pp. 1875–1888, Mar. 2010.

[26] H. Shin and J. B. Song, "MRC analysis of cooperative diversity with fixed-gain relays in Nakagami-*m* fading channels," *IEEE Trans. Wireless Commun.*, vol. 7, no. 6, pp. 2069–2074, Jun. 2008.

[27] C. D. Meyer, *Matrix Analysis and Applied Linear Algebra*. Philadelphia, PA, USA: SIAM, 2000.

[28] R. E. Prieto, "A general solution to the maximization of the multidimensional generalized Rayleigh quotient used in linear discriminant analysis for signal classification," in *Proc. IEEE Int. Conf. Acoust. Speech, Signal Process. (ICASSP)*, Hong Kong, Apr. 2003, pp. 157–160.

[29] J. Lee, H. Wang, J. G. Andrews, and D. Hong, "Outage probability of cognitive relay networks with interference constraints," *IEEE Trans. Wireless Commun.*, vol. 10, no. 2, pp. 390–395, Feb. 2011.

[30] J. Hoydis, S. ten Brink, and M. Debbah, "Massive MIMO in the UL/DL of cellular networks: How many antennas do we need?" *IEEE J. Sel. Areas Commun.*, vol. 31, no. 2, pp. 160–171, Feb. 2013.

[31] H. A. Suraweera, H. Q. Ngo, T. Q. Duong, C. Yuen, and E. G. Larsson, "Multi-pair amplify-and-forward relaying with very large antenna arrays," in *Proc. IEEE Int. Conf. Commun. (ICC)*, Budapest, Hungary, Jun. 2013, pp. 4635–4640.

[32] J. Hu, W. Yang, N. Yang, X. Zhou, and Y. Cai, "On–off-based secure transmission design with outdated channel state information," *IEEE Trans. Veh. Technol.*, vol. 65, no. 8, pp. 6075–6088, Aug. 2016.

Tiep M. Hoang (S'17) was born in Daklak, Vietnam, in 1989. He received the B.S. degree in electronics and electrical engineering from the Ho Chi Minh City University of Technology, Vietnam, in 2012, and the M.S. degree in electronics and radio engineering from Kyung Hee University, Seoul, South Korea, in 2014. He is currently pursuing the Ph.D. degree with the School of Electronics, Electrical Engineering and Computer Science, Queen's University Belfast, U.K. Since 2015, he has been a Research Assistant with Duy Tan University, Danang, Vietnam. His current research interests include wireless security, massive MIMO, and stochastic geometry.

Trung Q. Duong (S'05–M'12–SM'13) received the Ph.D. degree in telecommunications systems from the Blekinge Institute of Technology, Sweden, in 2012. Since 2013, he has been with the Queen's University Belfast, U.K., as a Lecturer (Assistant Professor). He has authored or co-authored over 250 technical papers in scientific journals (140 articles) and presented at international conferences (120 papers). His current research interests include small-cell networks, ultra-dense networks, physical layer security, energy-harvesting communications, and massive MIMO.

He received the Best Paper Award at the IEEE Vehicular Technology Conference in 2013, the IEEE International Conference on Communications 2014, and the IEEE Global Communications Conference 2016. He is a recipient of prestigious Royal Academy of Engineering Research Fellowship (2016–2021). He currently serves as an Editor for the IEEE TRANSACTIONS ON WIRELESS COMMUNICATIONS, the IEEE TRANSACTIONS ON COMMUNICATIONS, and *IET Communications*, and a Senior Editor of the IEEE COMMUNICATIONS LETTERS.

Hoang Duong Tuan received the Diploma (Hons.) and Ph.D. degrees in applied mathematics from Odessa State University, Ukraine, in 1987 and 1991, respectively. He spent nine academic years in Japan as an Assistant Professor with the Department of Electronic–Mechanical Engineering, Nagoya University, from 1994 to 1999, and then as an Associate Professor within the Department of Electrical and Computer Engineering, Toyota Technological Institute, Nagoya, from 1999 to 2003. He was a Professor with the School of Electrical Engineering and Telecommunications, University of New South Wales, from 2003 to 2011. He is currently a Professor with the Faculty of Engineering and Information Technology, University of Technology Sydney. He has been involved in research with the areas of optimization, control, signal processing, wireless communication, and biomedical engineering for over 20 years.

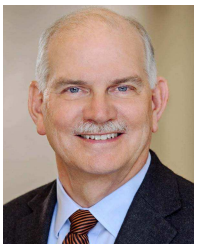

H. Vincent Poor (S'72–M'77–SM'82–F'87) received the Ph.D. degree in EECS from Princeton University in 1977. From 1977 to 1990, he was on the faculty of the University of Illinois at Urbana–Champaign. Since 1990, he has been on the faculty at Princeton, where he is currently the Michael Henry Strater University Professor of Electrical Engineering. From 2006 to 2016, he served as the Dean of Princeton's School of Engineering and Applied Science. His research interests are in the areas of information theory, signal processing, and their applications in wireless networks and related fields, such as smart grid and social networks. Among his publications in these areas is the book *Information Theoretic Security and Privacy of Information Systems* (Cambridge University Press, 2017).

Dr. Poor is a member of the National Academy of Engineering and the National Academy of Sciences, and is a foreign member of the Royal Society. He is also a fellow of the American Academy of Arts and Sciences, the National Academy of Inventors, and other national and international academies. He received the Marconi and Armstrong Awards of the IEEE Communications Society in 2007 and 2009, respectively. Recent recognition of his work includes the 2016 John Fritz Medal, the 2017 IEEE Alexander Graham Bell Medal, Honorary Professorships at Peking University and Tsinghua University, both conferred in 2016, and a D.Sc. *honoris causa* from Syracuse University in 2017.